THE JOURNAL OF COMPARATIVE NEUROLOGY 436:430–455 (2001)

Basic Organization of Projections From the Oval and Fusiform Nuclei of the Bed Nuclei of the Stria Terminalis in Adult Rat Brain

HONG-WEI DONG,[1,2] GORICA D. PETROVICH,[3] ALAN G. WATTS,[1] AND LARRY W. SWANSON[1]*

[1]Neuroscience Program and Department of Biological Sciences, University of Southern California, Los Angeles, California 90089-2520

[2]Institute of Neuroscience, The Fourth Military Medical University, Xi'an, Shannxi 710032, China

[3]Department of Psychology, Johns Hopkins University, Baltimore, Maryland 21218

ABSTRACT

The organization of axonal projections from the oval and fusiform nuclei of the bed nuclei of the stria terminalis (BST) was characterized with the *Phaseolus vulgaris*-leucoagglutinin (PHAL) anterograde tracing method in adult male rats. Within the BST, the oval nucleus (BSTov) projects very densely to the fusiform nucleus (BSTfu) and also innervates the caudal anterolateral area, anterodorsal area, rhomboid nucleus, and subcommissural zone. Outside the BST, its heaviest inputs are to the caudal substantia innominata and adjacent central amygdalar nucleus, retrorubral area, and lateral parabrachial nucleus. It generates moderate inputs to the caudal nucleus accumbens, parasubthalamic nucleus, and medial and ventrolateral divisions of the periaqueductal gray, and it sends a light input to the anterior parvicellular part of the hypothalamic paraventricular nucleus and nucleus of the solitary tract. The BSTfu displays a much more complex projection pattern. Within the BST, it densely innervates the anterodorsal area, dorsomedial nucleus, and caudal anterolateral area, and it moderately innervates the BSTov, subcommissural zone, and rhomboid nucleus. Outside the BST, the BSTfu provides dense inputs to the nucleus accumbens, caudal substantia innominata and central amygdalar nucleus, thalamic paraventricular nucleus, hypothalamic paraventricular and periventricular nuclei, hypothalamic dorsomedial nucleus, perifornical lateral hypothalamic area, and lateral tegmental nucleus. Moderately dense inputs are found in the parastrial, tuberal, dorsal raphé, and parabrachial nuclei and in the retrorubral area, ventrolateral division of the periaqueductal gray, and pontine central gray. Light projections end in the olfactory tubercle, lateral septal nucleus, posterior basolateral amygdalar nucleus, supramammillary nucleus, and nucleus of the solitary tract. These and other results suggest that the BSTov and BSTfu are basal telencephalic parts of a circuit that coordinates autonomic, neuroendocrine, and ingestive behavioral responses during stress. J. Comp. Neurol. 436:430–455, 2001.

Indexing terms: autonomic; central amygdalar nucleus; CRH; ingestive behavior; paraventricular nucleus of the hypothalamus; stress

Many studies indicate that the bed nuclei of the stria terminalis (BST) play an important role in the coordination of neuroendocrine, autonomic, and somatomotor responses during behaviors associated with a definite affective or emotional component (Casada and Dafny, 1991; Swanson, 1991; Gray et al., 1993; Dunn and Williams, 1995; Herman and Cullinan, 1997; Risold et al., 1997; Watts, 2001). The BST receive massive, topographically organized inputs from most parts of the amygdala (Krettek and Price, 1978; Weller and Smith, 1982; Dong et al., 2001) and in turn project massively to the nucleus accumbens (ventral striatum), substantia innominata (ventral pallidum), hypothalamus, midline thalamic nuclei, and

Contract grant sponsor: National Institutes of Health; Contract grant number: 2R01NS16686; Contract grant number: NS29728; Contract grant number: NSKO401833.

*Correspondence to: Dr. L.W. Swanson, Hedco Neuroscience Building, Rm. 428, University of Southern California, Los Angeles, CA 90089-2520. E-mail: lswanson@usc.edu

Received 13 February 2001; Revised 3 April 2001; Accepted 15 May 2001

Abbreviations

AAA	anterior amygdalar area
ac	anterior commissure
ACB	nucleus accumbens
aco	anterior commissure, olfactory limb
act	anterior commissure, temporal limb
ADP	anterodorsal nucleus thalamus
AHA	anterior hypothalamic area
AHN	anterior hypothalamic nucleus
AHNa	anterior hypothalamic nucleus, anterior part
AHNc	anterior hypothalamic nucleus, central part
AHNd	anterior hypothalamic nucleus, dorsal part
AHNp	anterior hypothalamic nucleus, posterior part
AMd	anteromedial nucleus thalamus, dorsal part
AP	area postrema
AQ	cerebral aqueduct
ARH	arcuate nucleus hypothalamus
AVP	anteroventral preoptic nucleus
AVPV	anteroventral periventricular nucleus hypothalamus
B	Barrington's nucleus
BA	bed nucleus accessory olfactory tract
BLAa	basolateral amygdalar nucleus, anterior part
BLAp	basolateral amygdalar nucleus, posterior part
BMAa	basomedial amygdalar nucleus, anterior part
BMAp	basomedial amygdalar nucleus, posterior part
BST	bed nuclei of the stria terminalis
BSTad	bed nuclei of the stria terminalis, anterior division, anterodorsal area
BSTal	bed nuclei of the stria terminalis, anterior division, anterolateral area
BSTav	bed nuclei of the stria terminalis, anterior division, anteroventral area
BSTcc	bed nuclei of the stria terminalis, anterior division, anterodorsal area, central core
BSTd	bed nuclei of the stria terminalis, posterior division, dorsal nucleus
BSTdl	bed nuclei of the stria terminalis, anterior division, dorsolateral nucleus
BSTdm	bed nuclei of the stria terminalis, anterior division, dorsomedial nucleus
BSTfu	bed nuclei of the stria terminalis, anterior division, fusiform nucleus
BSTif	bed nuclei of the stria terminalis, posterior division, interfascicular nucleus
BSTju	bed nuclei of the stria terminalis, anterior division, juxtacapsular nucleus
BSTmg	bed nuclei of the stria terminalis, anterior division, magnocellular nucleus
BSTov	bed nuclei of the stria terminalis, anterior division, oval nucleus
BSTpr	bed nuclei of the stria terminalis, posterior division, principal nucleus
BSTrh	bed nuclei of the stria terminalis, anterior division, rhomboid nucleus
BSTsc	bed nuclei of the stria terminalis, anterior division, subcommissural zone
BSTse	bed nuclei of the stria terminalis, posterior division, stria extension
BSTsz	bed nuclei of the stria terminalis, posterior division, cell-sparse zone
BSTtr	bed nuclei of the stria terminalis, posterior division, transverse nucleus
BSTv	bed nuclei of the stria terminalis, anterior division, ventral nucleus
CA1	field CA1, ammon's horn
CA2	field CA2, ammon's horn
CA3	field CA3, ammon's horn
CEA	central nucleus amygdala
CEAc	central nucleus amygdala, capsular part
CEAl	central nucleus amygdala, lateral part
CEAm	central nucleus amygdala, medial part
CLI	central linear nucleus raphé
CM	central medial nucleus thalamus
COAa	cortical nucleus amygdala, anterior part
COApl	cortical nucleus amygdala, posterior part, lateral zone
COApm	cortical nucleus amygdala, posterior part, medial zone
COM	commissural nucleus, periaqueductal gray
CP	caudoputamen
cpd	cerebral peduncle
CSm	superior central nucleus raphé, medial part
CUN	cuneiform nucleus
DMH	dorsomedial nucleus hypothalamus
DMHa	dorsomedial nucleus hypothalamus, anterior part
DMHp	dorsomedial nucleus hypothalamus, posterior part
DMHv	dorsomedial nucleus hypothalamus, ventral part
DMX	dorsal motor nucleus vagus nerve
DR	dorsal nucleus raphé
DTN	dorsal tegmental nucleus
ENTl	entorhinal area, lateral part
EPv	endopiriform nucleus, ventral part
EW	Edinger-Westphal nucleus
FF	fields of Forel
fi	fimbria
fr	fasciculus retroflexus
FS	fundus of the striatum
fx	columns of the fornix
GP	globus pallidus
GPl	globus pallidus, lateral segment
GPm	globus pallidus, medial segment
GR	gracile nucleus
GRN	gigantocellular reticular nucleus
IA	intercalated nuclei amygdala
IAM	interanteromedial nucleus thalamus
ic	internal capsule
IC	inferior colliculus
ICc	inferior colliculus, central nucleus
ICe	inferior colliculus, external nucleus
IF	interfascicular nucleus
ILA	infralimbic cortical area
IMD	intermediodorsal nucleus thalamus
INS	insular cortical area
int	internal capsule
isl	islands of Calleja (olfactory tubercle)
IVn	trochlear nerve
KF	Kölliker-Fuse subnucleus (of PB)
LA	lateral amygdalar nucleus
LC	locus coeruleus
LDT	laterodorsal tegmental nucleus
LH	lateral habenula
LHA	lateral hypothalamic area
LM	lateral mammillary nucleus
LPO	lateral preoptic area
LS	lateral septal nucleus
LSc	lateral septal nucleus, caudal part
LSr	lateral septal nucleus, rostral part
LSr.vl.v.	lateral septal nucleus, rostral part, ventrolateral zone, ventral region
LSv	lateral septal nucleus, ventral part
LTN	lateral tegmental nucleus
LV	lateral ventricle
MA	magnocellular preoptic nucleus
MD	mediodorsal nucleus thalamus
MDc	mediodorsal nucleus thalamus, central part
MDl	mediodorsal nucleus thalamus, lateral part
MDm	mediodorsal nucleus thalamus, medial part
MEAad	medial nucleus amygdalar, anterodorsal part
MEApd	medial nucleus amygdalar, posterodorsal part
MEApv	medial nucleus amygdalar, posteroventral part
MEPO	median preoptic nucleus
MEV	mesencephalic nucleus of the trigeminal
ml	medial lemniscus
mlf	medial longitudinal fascicle
MM	medial mammillary nucleus
moV	motor root of the trigeminal nerve
mp	mammillary peduncle
MPN	medial preoptic nucleus
MPO	medial preoptic area
MRN	mesencephalic reticular nucleus
MS	medial septal nucleus
mtt	mammillothalamic tract
mtV	mesencephalic tract of the trigeminal nerve
NDB	nucleus of the diagonal band
NLOT	nucleus of the lateral olfactory tract
NTS	nucleus of solitary tract
NTSce	nucleus of the solitary tract, central part
NTSge	nucleus of the solitary tract, gelatinous part
NTSl	nucleus of solitary tract, lateral part
NTSm	nucleus of solitary tract, medial part

Abbreviations (continued)

och	optic chiasm
opt	optic tract
OT	olfactory tubercle
OV	vascular organ of the lamina terminalis
PA	posterior nucleus amygdala
PAG	periaqueductal gray
PAGd	periaqueductal gray, dorsal division
PAGdl	periaqueductal gray, dorsolateral division
PAGm	periaqueductal gray, medial division
PAGrl	periaqueductal gray, rostrolateral division
PAGrm	periaqueductal gray, rostromedial division
PAGvl	periaqueductal gray, ventrolateral division
PARN	parvicellular reticular nucleus
PB	parabrachial nucleus
PBl	parabrachial nucleus, lateral division
PBlc	parabrachial nucleus, central lateral part
PBld	parabrachial nucleus, dorsal lateral part
PBle	parabrachial nucleus, external lateral part
PBlv	parabrachial nucleus, ventral lateral part
PBm	parabrachial nucleus, medial division
PBme	parabrachial nucleus, external medial part
PBmm	parabrachial nucleus, medial medial part
PCG	pontine central gray
PF	parafascicular nucleus
PH	posterior hypothalamic nucleus
PL	prelimbic cortical area
pm	principal mammillary tract
PMv	ventral premammillary nucleus
PPN	pedunculopontine nucleus
PR	perireuniens nucleus
PRC	precommissure nucleus, periaqueductal gray
PRN	pontine reticular nucleus
PRNc	pontine reticular nucleus, caudal part
PRNr	pontine reticular nucleus, rostral part
PS	parastrial nucleus
PSCH	suprachiasmatic preoptic nucleus
PT	parataenial nucleus
PVa	anterior periventricular nucleus hypothalamus
PVH	paraventricular nucleus hypothalamus
PVHam	paraventricular nucleus hypothalamus, anterior magnocellular part
PVHap	paraventricular nucleus hypothalamus, anterior parvicellular part
PVHd	paraventricular nucleus hypothalamus, descending division
PVHdp	paraventricular nucleus hypothalamus, dorsal parvicellular part
PVHf	paraventricular nucleus hypothalamus, forniceal part
PVHlp	paraventricular nucleus hypothalamus, lateral parvicellular part
PVHm	paraventricular nucleus hypothalamus, magnocellular division
PVHmm	paraventricular nucleus hypothalamus, medial magnocellular part
PVHmp	paraventricular nucleus hypothalamus, medial parvicellular part
PVHmpd	paraventricular nucleus hypothalamus, medial parvicellular part, dorsal zone
PVHmpv	paraventricular nucleus hypothalamus, medial parvicellular part, ventral zone
PVHp	paraventricular nucleus hypothalamus, parvicellular division
PVHpm	paraventricular nucleus hypothalamus, posterior magnocellular part
PVHpml	paraventricular nucleus hypothalamus, posterior magnocellular part, lateral zone
PVHpmm	paraventricular nucleus hypothalamus, posterior magnocellular part, medial zone
PVHpv	paraventricular nucleus hypothalamus, periventricular part
PVi	intermediate periventricular nucleus hypothalamus
PVp	posterior periventricular nucleus hypothalamus
PVpo	preoptic periventricular nucleus
PVT	paraventricular nucleus thalamus
RCH	retrochiasmatic area
RE	nucleus reuniens
REa	nucleus reuniens, rostral division, anterior part
REc	nucleus reuniens, caudal division, caudal part
REcd	nucleus reuniens, caudal division, dorsal part
REcm	nucleus reuniens, caudal division, median part
REd	nucleus reuniens, rostral division, dorsal part
REl	nucleus reuniens, rostral division, lateral part
REm	nucleus reuniens, rostral division, medial part
REr	nucleus reuniens, rostral division
RH	rhomboid nucleus
RL	rostral linear nucleus raphé
RN	red nucleus
RR	mesencephalic reticular nucleus, retrorubral area
RT	reticular nucleus thalamus
SBPV	subparaventricular zone hypothalamus
SC	superior colliculus
SCH	suprachiasmatic nucleus
SCP	superior cerebellar peduncle
SF	septofimbrial nucleus
SI	substantia innominata
sm	stria medullaris
SN	substantia nigra
SNc	substantia nigra, compact part
SNr	substantia nigra, reticular part
SO	supraoptic nucleus
SPF	subparafascicular nucleus thalamus
SPFm	subparafascicular nucleus thalamus, magnocellular part
SPFp	subparafascicular nucleus thalamus, parvicellular part
st	stria terminalis
STN	subthalamic nucleus
SUBv	subiculum, ventral part
SUM	supramammillary nucleus
SUMl	supramammillary nucleus, lateral part
SUMm	supramammillary nucleus, medial part
SUT	supratrigeminal nucleus
TM	tuberomammillary nucleus
TMd	tuberomammillary nucleus, dorsal part
TMv	tuberomammillary nucleus, ventral part
TR	postpiriform transition area
TRS	triangular nucleus septum
TTd	taenia tecta, dorsal part
TU	tuberal nucleus
V3	third ventricle
V4	fourth ventricle
VL	lateral ventricle
VMH	ventromedial nucleus hypothalamus
VMHa	ventromedial nucleus hypothalamus, anterior part
VMHc	ventromedial nucleus hypothalamus, central part
VMHdm	ventromedial nucleus hypothalamus, dorsomedial part
VMHvl	ventromedial nucleus hypothalamus, ventrolateral part
VPMpc	ventral posteromedial nucleus, parvicellular part
VTA	ventral tegmental area
ZI	zona incerta
ZIda	zona incerta, dopaminergic group
zl	zona limitans

brainstem nuclei related to autonomic and somatomotor activities (Swanson and Cowan, 1979; Schwaber et al., 1982; Sofroniew, 1983; Holstege et al., 1985; Risold et al., 1997; Dong et al., 1999, 2000).

Originally, the BST were parceled into medial and lateral divisions based mainly on their amygdalar inputs. The former was characterized by inputs from the medial nucleus, whereas the latter was characterized by inputs from the central (CEA) and basolateral nuclei (Bleier, 1961; de Olmos, 1972; Krettek and Price, 1978), and more detailed variations on this basic medial/lateral division are still widely used (Ricardo, 1978; Schwaber et al., 1982; Weller and Smith 1982; Sofroniew, 1983; van der Kooy et al., 1984; de Olmos et al., 1985; Holstege, 1985; Alden et al., 1994; Alheid et al., 1995; Paxinos and Watson, 1998). In contrast, developmental evidence suggests a funda-

mental anterior/posterior (rostral/caudal) division (Bayer, 1987), and Ju and his colleagues (1989a,b) independently arrived at the same conclusion based on cyto- and chemoarchitectonic observations in the adult rat. The latter authors further parceled the adult anterior division into dorsal, lateral, and ventral areas, and within them 12 distinct cell groups (nuclei) were identified. Our previous work has shown that the juxtacapsular (BSTju) and rhomboid (BSTrh) nuclei in the lateral area of the anterior BST display unique projection patterns (Dong et al., 1999, 2000), although projections from the BSTov—another distinct part of the lateral area of the anterior BST—remain to be clarified.

The BSTov, together with the nearby BSTfu, have attracted considerable attention in the last decade. Both cell groups contain abundant γ-aminobutyric acid (GABA)-ergic neurons (Le Gal La Salle et al., 1978; Nitecka and Ben-Ari, 1987; Sun and Cassell, 1993; Risold and Swanson, 1997; Day et al., 1999), many of which also express corticotropin-releasing hormone (CRH; Ju et al., 1989; Watts et al., 1995; Day et al., 1999). This is interesting because nonneuroendocrine CRH neurons have been implicated in behavioral responses to stress, fear, and anxiety (Dallman et al., 1987; Dunn and Berridge, 1990; Koob et al., 1993). Infusion of CRH into the lateral ventricle produces behavioral responses similar to those associated with conditioned fear (Dunn and Berridge, 1990; Koob et al., 1993), but, more specifically, microinfusion of CRH directly into the BST mimics some of these effects. Furthermore, microinfusion of CRH antagonist into the BST blocks ventricular CRH-enhanced startle responses in a dose-dependent manner (Lee and Davis, 1997), and lesions of the "lateral part of BST" (which includes our BSTov and BSTfu) attenuate the effects of CRH infused into the lateral ventricle (Gray et al., 1993).

Perhaps of even greater interest is that the lateral part of the central amygdalar nucleus (CEAl), which also contains many GABAergic neurons that express CRH (Veening et al., 1984; Nitecka and Ben-Ari, 1987; Sun and Cassell, 1993; Watts et al., 1995; Day et al., 1999), projects in a very dense and selective way to both the BSTov and the BSTfu (Petrovich and Swanson, 1997). This evidence, combined with the fact that CRH mRNA levels in the CEA (Swanson and Simmons, 1989; Watts and Sanchez-Watts, 1995) and in the BSTov and BSTfu (Markino et al., 1994; Watts and Sanchez-Watts, 1995) may be regulated to greater or lesser degrees by corticosterone, has led to the suggestion that all three nuclei form part of an adrenal steroid-sensitive network involved in regulating the output of the medial part of the central amygdalar nucleus (CEAm; Petrovich and Swanson, 1997).

Unfortunately, the outputs of the BSTov and BSTfu themselves remain essentially unknown, in part because previous anterograde tracing experiments, based on the autoradiographic method, inevitably produced injection sites that were much too large (Swanson and Cowan, 1979; Holstege et al., 1985). Thus, we decided to characterize their overall projections with the anterograde tracer *Phaseolus vulgaris*-leucoagglutinin (PHAL), because it produces small injection sites and is very sensitive. The intent is to provide a starting point for more detailed analysis with retrograde tracer, histochemical, ultrastructural, and physiological methods.

MATERIALS AND METHODS

Experiments were performed in accordance with the NIH Guidelines for the Care and Use of Laboratory Animals, and all protocols were approved by the University of Southern California Institutional Animal Care and Use Committee. A total of 30 adult male Harlan Sprague-Dawley rats (300–350 g) received a single, stereotaxically placed iontophoretic injection of a 2.5% solution of PHAL (Vector Laboratories, Burlingame, CA), prepared in 0.01 M sodium phosphate-buffered saline (pH 7.4; NaPBS), into the region of the BSTov or BSTfu through a glass micropipette (15 μm tip diameter) by applying a positive current (5 μA, 7 sec on/off intervals) for 7–10 min. Animals were anesthetized for stereotaxic surgery with an equal mixture of ketamine and xylazine solutions (50 mg/ml ketamine, 10 mg xylazine/ml; 1 ml/kg body weight).

After a survival time of 14–16 days, the rats were deeply anesthetized with pentobarbital (40 mg/kg body weight intraperitoneally) and perfused transcardially with 150 ml of 0.9% NaCl followed by 300 ml of ice-cold 4% paraformaldehyde in 0.1 M borate buffer, pH 9.5. The brains were removed, postfixed overnight at 4°C in the same fixative containing 10% sucrose, and frozen. Then, serial 30 μm-thick sections (1 in 4) were cut in the transverse plane on a sliding microtome. One complete series of sections was processed to detect PHAL using the immunohistochemical procedure described elsewhere (Gerfen and Sawchenko, 1984; Petrovich and Swanson, 1997). PHAL-containing cells (in the injection sites) and fibers were plotted with the aid of a camera lucida onto cytoarchitectonic drawings of adjacent thionin-stained sections and then transferred onto a series of standard drawings of the rat brain (Swanson, 1999) with the aid of a computer (Apple Power Mac G4, Adobe Illustrator 9). Parceling of the rat brain, and the terminology for describing morphological features of PHAL-labeled axons, follows Swanson (1999), unless indicated otherwise.

Another adjacent series of 30 μm-thick sections through the PHAL injection site was collected into ice-cold KPBS containing 0.25% paraformaldehyde and mounted immediately onto gelatin-coated/poly(L)-lysine-coated slides, vacuum desiccated overnight, and stored at –70°C for CRH mRNA hybridization histochemistry. This histochemistry was done to provide a chemoarchitectonic marker for the BSTov and BSTfu.

For in situ hybridization, ^{35}S-labeled riboprobe complementary to CRH mRNA was prepared using a Promega Gemini Kit (Promega Inc., Madison, WI) exactly as described previously (Watts and Sanchez-Watts, 1995). Briefly, slides were pretreated for 1 hour each in 4% paraformaldehyde/potassium phosphate-buffered saline, pH 7.4, then proteinase K, dehydrated through ascending concentrations of ethanol, and vacuum desiccated. Slides were hybridized by using a 700-base-pair CRH cRNA probe kindly provided by Dr. Joseph Majzoub (Frim et al., 1990) at 60°C for 18–20 hours. After hybridization, sections were treated with RNase, washed in descending concentrations of saline-sodium citrate buffer, and then dehydrated through ascending concentrations of ethanol. Slides were air dried and exposed to Cronex Microvision X-ray film (Dupont, Wilmington, DE) for 1–10 days, dipped in liquid photographic emulsion (Kodak NTB-2, diluted 1:1 with water), exposed for 7–11 days, and developed.

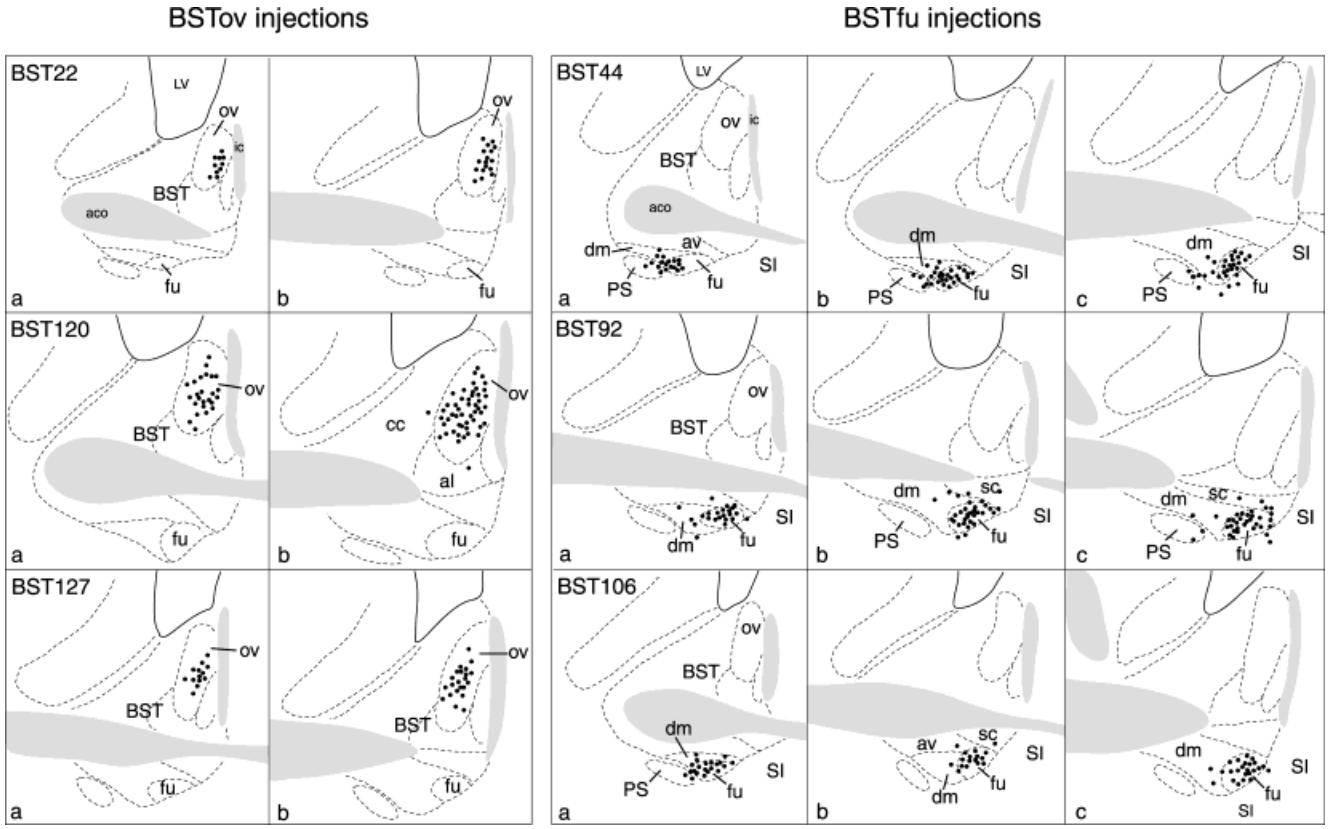

Fig. 1. Cameral lucida plots of histological sections with labeled neurons (black dots) following PHAL injections into the BSTov (experiments BST22, BST120, and BST127) and BSTfu (experiments BST44, BST92, and BST106). In each case, a is rostral to b and, then, c.

RESULTS

Nomenclature

Before describing the projections of the BSTov and BSTfu, it is important to consider the boundaries adopted here for these cell groups, because different nomenclatures have been used in the past and no real consensus has emerged. The BSTov (Ju and Swanson, 1989; Ju et al., 1989) is a roughly oval, compact cell group that is centered in midrostrocaudal levels of the anterolateral area, where it lies dorsally, just medial to the internal capsule and lateral to the anterodorsal area (Fig. 1). It corresponds roughly to the "dorsal part of the lateral BST" (BSTLD) of de Olmos et al. (1985), Paxinos and Watson (1986), and Alheid et al. (1995) and to the "dorsal lateral subnucleus of the lateral BST" (BSTDL) of Moga et al. (1989); it is included in the "anterolateral subdivision" of the BST of Weller and Smith (1982) and Sun and Cassell (1993). In most other work, it probably lies within the "lateral part of the BST" (e.g., Krettek and Price, 1978; Schwaber et al., 1982; Sofroniew, 1983).

The BSTfu is a small but relatively well-defined cell group that lies along the ventromedial border of the anterolateral area (Dong et al., 2001; Fig. 1). It is bordered dorsomedially by the dorsomedial nucleus of the BST, dorsolaterally by the subcommissural zone of the BST, and medially by the parastrial nucleus of the preoptic region. It begins rostrally at about the same level as the parastrial nucleus, and then shifts laterally, almost reaching the lateral edge of the BST caudally. The cluster of cells was marked, but not labeled, in the atlas of Paxinos and Watson (1986). It corresponds well to the lateral division, ventral (LV) of the BST according to de Olmos (1985) and to the ventral lateral subnucleus of the BST (BSTvl) according to Moga et al. (1989). However, the "ventral lateral part of the BST" indicated in some studies (e.g., Alden et al., 1994) also includes our subcommissural zone of the BST, which appears to generate an output pattern that is distinct from the BSTfu (see below). Recently, "fusiform nucleus" as described here has been adopted by Alheid et al. (1995) and Paxinos and Watson (1998).

Projections from the BSTov

In seven experiments, the PHAL injection was centered in the BSTov, and three of the injection sites were very small and apparently restricted entirely (Fig. 1, experiments BST22, BST127) or almost entirely (Fig. 1, experiment 120) to the nucleus. The other four injection sites were larger, and a few PHAL-labeled neurons spread into adjacent regions of the BST (not shown here). The borders of the BSTov were confirmed in adjacent Nissl-stained sections, and in adjacent sections hybridized for CRH mRNA, because it is abundantly expressed in BSTov neurons but is much less abundant in surrounding areas (Fig.

2C). The projections labeled in experiment BST120 are illustrated in detail because it has the largest injection site virtually limited to the BSTov (Figs. 1, 2A–C) and because the projection pattern (Figs. 3, 4A–W) is indistinguishable from that in the other experiments with a PHAL injection essentially restricted to the BSTov. Overall, our results suggest that the BSTov displays a relatively simple pattern of projections to other regions of the basal telencephalon, hypothalamus, and lower brainstem (Fig. 5).

Local projections. Although the longer projections of the BSTov are relative simple, its short, local inputs are rather more complex. From the injection site a few PHAL-labeled axons extend rostrally and generate a small number of terminal boutons in the rostral anterolateral area of the BST (Fig. 4C), and a distinct bundle of labeled axons streams ventrally through the subcommissural zone of the BST to provide an extremely dense input to the BSTfu, where the PHAL-labeled axons branch profusely and display very dense terminal boutons (Figs. 2B, 4D). Then, many of these PHAL-labeled axons appear to extend rostrally through the dorsomedial nucleus and anteroventral area, arch around the medial edge of the anterior commissure, and enter the anterodorsal area of the BST (Fig. 4B–D). Moderate numbers of terminal boutons were observed in the subcommissural zone and anterodorsal area, whereas only a few boutons-of-passage were observed in the dorsomedial nucleus and anteroventral area of the BST (Fig. 4B–D). More rostrally, these axons from the BSTov provide a moderately dense input to the most caudal region of the nucleus accumbens (Fig. 4A), just rostral to the BST. In addition, a very few PHAL-labeled axons were observed dorsally in the lateral margin of the lateral septal nucleus (Fig. 4A) and ventrally in the rostroventral substantia innominata (Fig. 4A–D).

The vast majority of PHAL-labeled axons from the BSTov extends caudally into the rhomboid nucleus, caudal anterolateral area, and far lateral regions of the interfascicular and transverse nuclei of the BST (Fig. 4E,F). These labeled axons generate a moderate number of terminal boutons and boutons-of-passage in the rhomboid nucleus of the BST, and very rich terminal fields in the caudoventral corner of the anterolateral area, and far lateral regions of the interfascicular and transverse nuclei of the BST (Fig. 4E,F). Small numbers of scattered fibers were also observed in the lateral or external segment of the globus pallidus (Fig. 4E,F). As we shall now see, descending projections from the BSTov appear to follow four distinct pathways to reach their terminal fields outside the BST.

Ansa peduncularis projection. A massive group of highly branched PHAL-labeled axons with very rich terminal boutons and varicosities extends from the caudoventral corner of the anterolateral area, and the lateral region of the interfascicular and transverse nuclei of the BST, into adjacent dorsolateral regions of the substantia innominata (Figs. 3A, 4E,F). This dense terminal field extends uninterrupted through the caudal substantia innominata from the level of the crossing of the anterior commissure to its caudal tip adjacent to the amygdala (Fig. 4E–H).

Caudally, this dense projection from the BSTov extends into the CEA, whereas the rest of the amygdala is almost free of PHAL labeling except for a few axons in the posterior basolateral nucleus and postpiriform transition area (Fig. 4K,L). The CEAm is very densely innervated by abundant, highly branched, bouton-laden fibers (Figs. 3B, 4G–I), whereas the lateral and capsular parts of the CEA display moderate numbers of fibers with terminal boutons, especially in more caudal levels (Fig. 4G–J).

Stria terminalis pathway. A small group of PHAL-labeled axons travels dorsally from the BSTov injection site to enter the stria terminals; they then follow it to the amygdala (Fig. 4E–J), where they cannot be distinguished from labeled axons arriving via the ansa peduncularis pathway described above.

Periventricular pathway. Small numbers of PHAL-labeled axons course medially though the anteroventral area, and the ventral and dorsomedial nuclei of the BST, to enter the periventricular zone of the hypothalamus just ventral to the region where the anterior commissure crosses the midline (Fig. 4E,F). These fibers terminate in the anterior parvicellular part of the paraventricular nucleus, and, interestingly, this appears to be the only region of the hypothalamic periventricular zone innervated by the BSTov (Fig. 4F).

Medial forebrain bundle pathway. Another group of PHAL-labeled axons from the BSTov courses medial to the substantia innominata and lateral preoptic area to enter the lateral hypothalamic area (Fig. 4E–I). These fibers descend through far lateral regions of the lateral hypothalamic area and for the most part appear to be fibers-of-passage, except for a few branches that seem to end in the perifornical region at tuberal levels (Fig. 4J) and a moderate number of branches with terminal boutons in the region just dorsomedial to the subthalamic nucleus (Fig. 4K), which was identified and named the "parasubthalamic nucleus" by Wang and Zhang (1995; see also Paxinos and Watson, 1998). At this level, a very few labeled fibers were found in the subthalamic nucleus and midline nuclei of the thalamus (Fig. 4J,K).

This group of descending fibers then courses through the ventral tegmental area, compact part of the substantia nigra, zona incerta, and mesencephalic reticular nucleus (Fig. 4L,M), where they display very few terminal boutons and are thus presumably fibers-of-passage, to provide a very dense input with very rich branches and terminal boutons in the retrorubral area (Fig. 4N,O). Then, a bundle of fibers arches caudally, dorsally, and then medially through the mesencephalic reticular nucleus to innervate moderately the ventrolat-

Fig. 2 (Overleaf). Darkfield photomicrographs illustrating the appearance of a PHAL injection site in the BSTov (**B**, experiment BST120; see corresponding section b in Fig. 1) and in the BSTfu (**B′**, experiment BST92; see corresponding section b in Fig. 1), along with the caudally adjacent thionin-stained transverse sections (**A, A′**, respectively). The rostrally adjacent sections were subjected to in situ hybridization for CRH mRNA (**C, C′**). Arrows point to the same blood vessels in the photomicrographs. Scale bars = 300 μm.

Fig. 3 (Overleaf). Darkfield photomicrographs showing the appearance of PHAL-labeled axons from the BSTov (A–C) and from the BSTfu (A′–E′) in the substantia innominata (SI; **A, A′**), in the central amygdalar nucleus (CEA; **B,B′**), and in the pontine central gray and parabrachial nucleus (PB; **C,C′**). In addition, the BSTfu sends dense projections to parts of the hypothalamus, including the paraventricular nucleus (PVH; **D′**) and the dorsomedial nucleus (DMH), and perifornical region of the lateral hypothalamic area (**E′**). Scale bars = 300 μm.

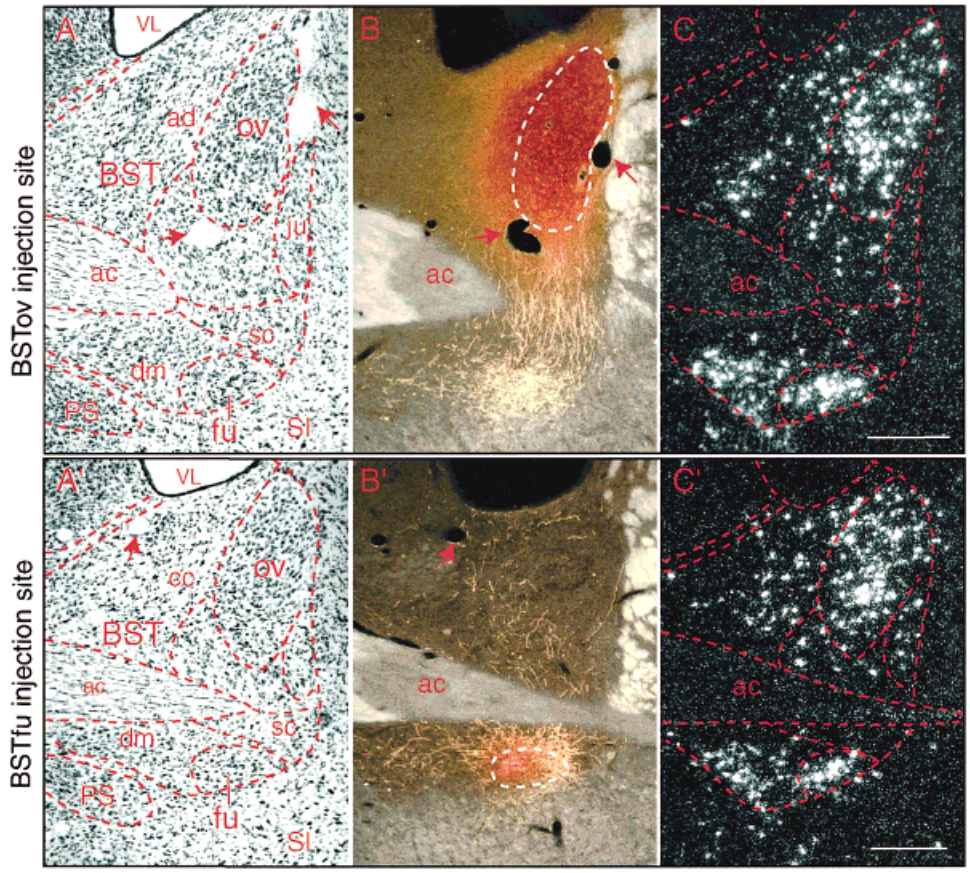

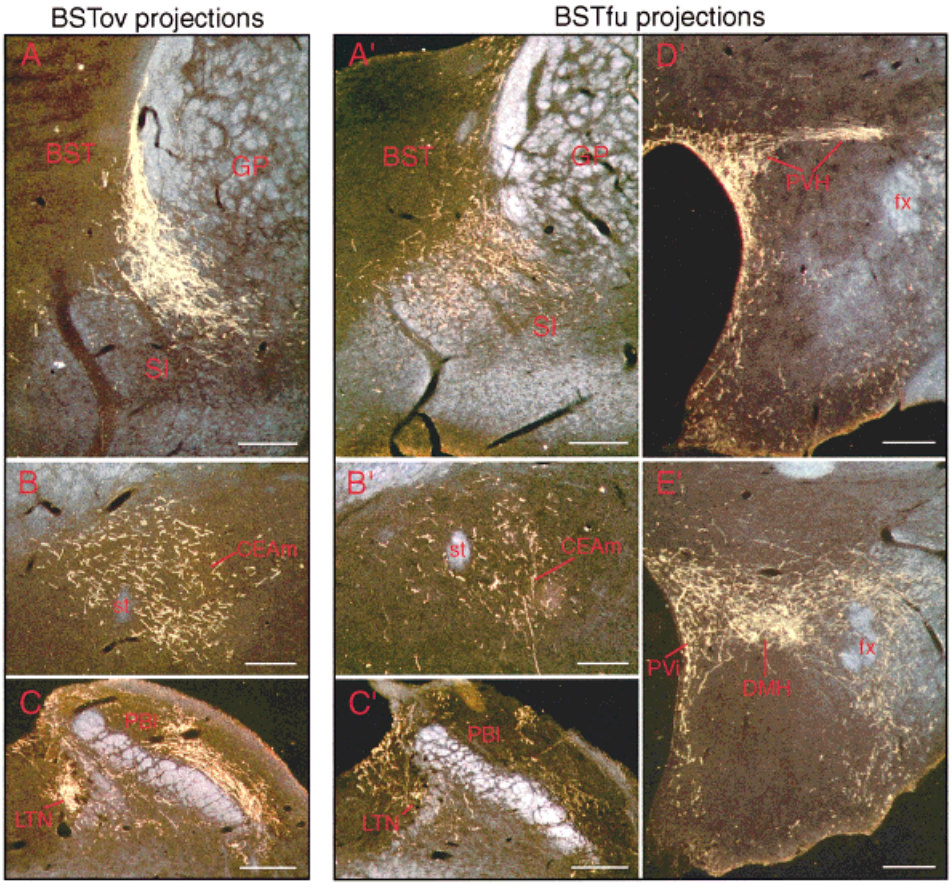

Figures 2 and 3

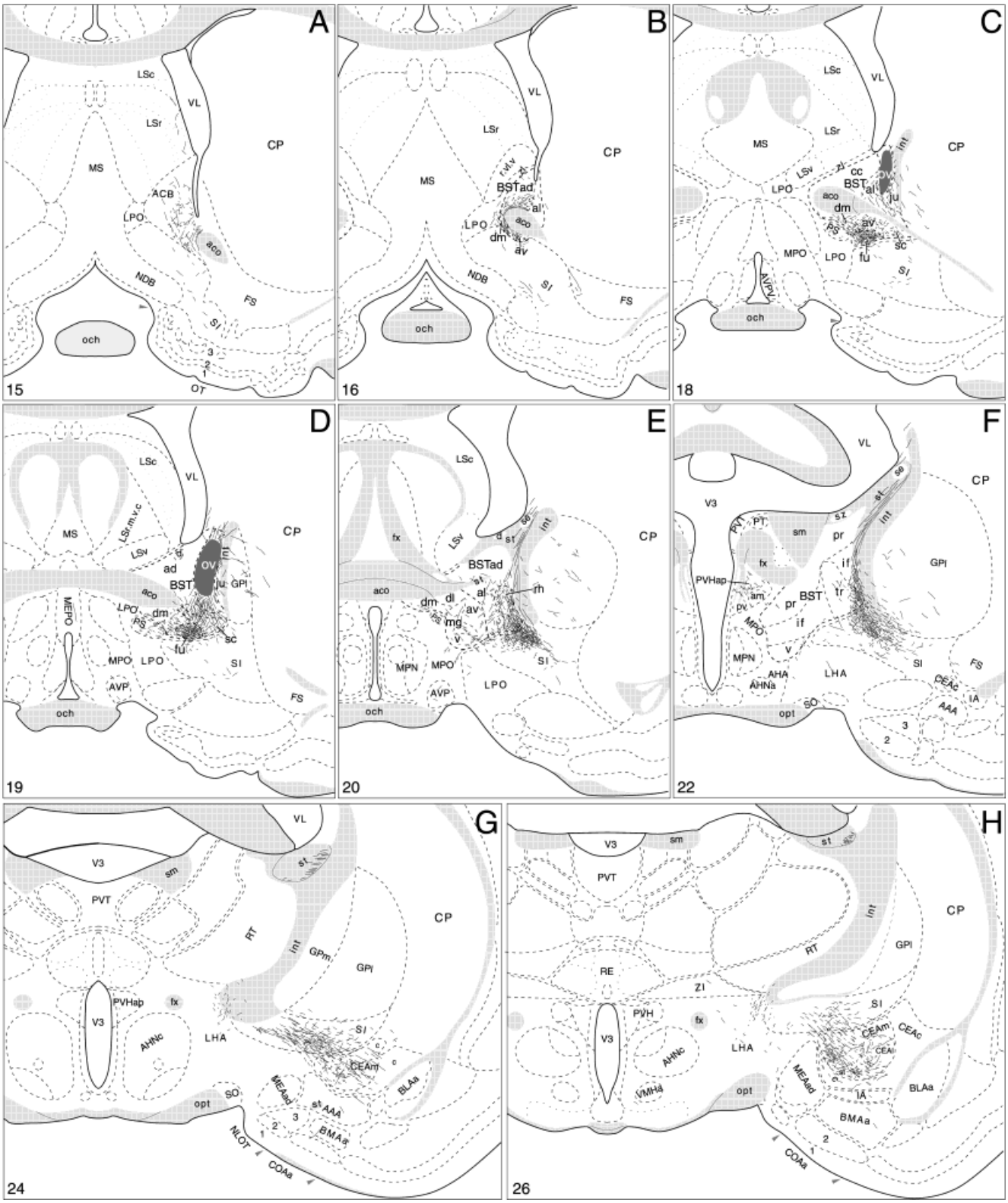

Fig. 4. Summary of BSTov projections. The distribution of PHAL-labeled axons in experiment BST120 was plotted onto a series of standard drawings of the rat brain derived from an atlas (Swanson, 1999), arranged from rostral (**A**) to caudal (**W**). The dark gray area in the BSTov (**D**) indicates the injection site (see Figs. 1, 2). The number in the lower left corner of each drawing refers to the corresponding rostrocaudal level of the atlas.

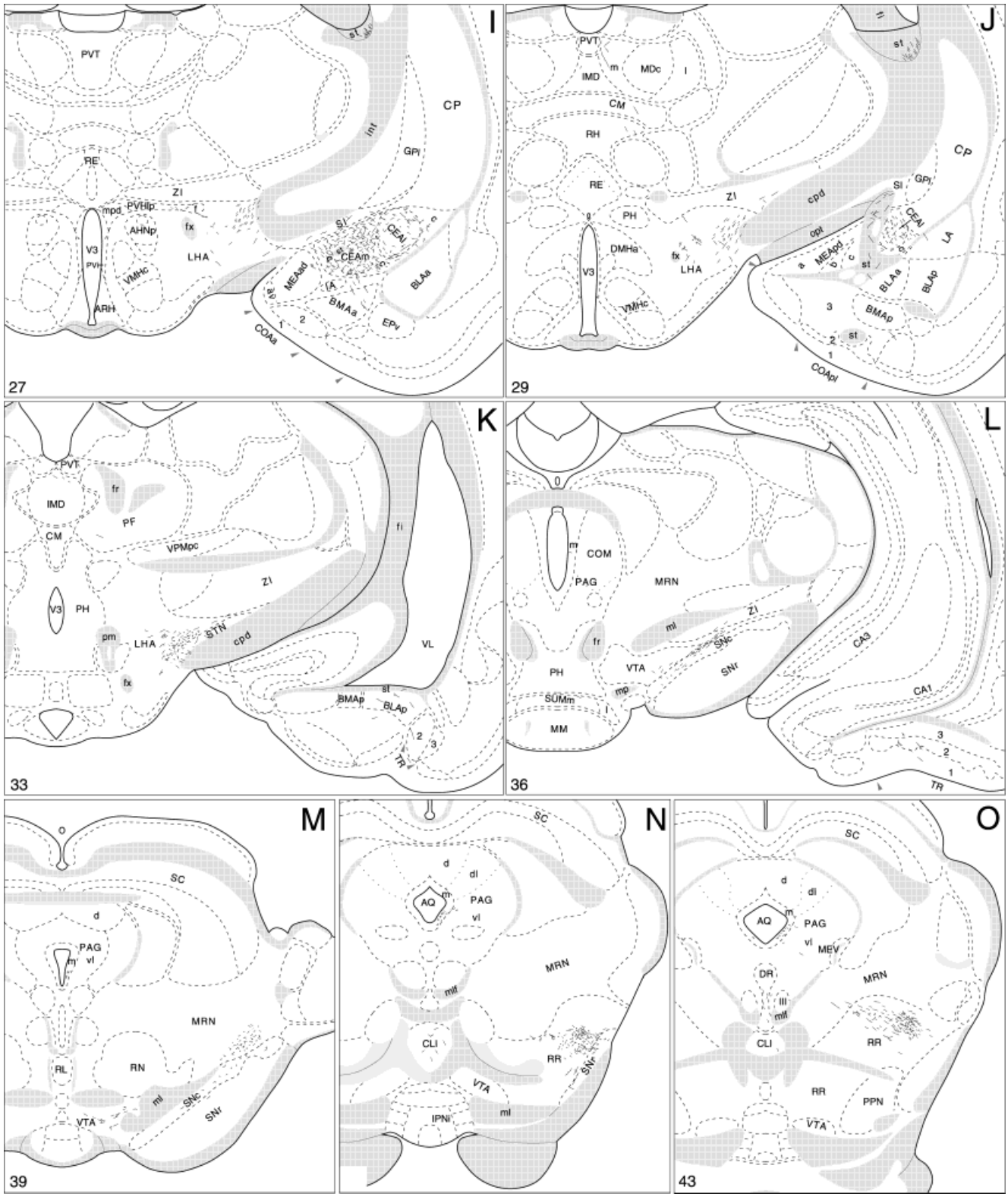

Figure 4 (Continued)

eral division of the periaqueductal gray (Fig. 4P). A few PHAL-labeled axons extend medially into the dorsal raphé nucleus and the contralateral ventrolateral periaqueductal gray (Fig. 4P), and even fewer axons were observed in the medial division of the periaqueductal gray (Fig. 4K–P).

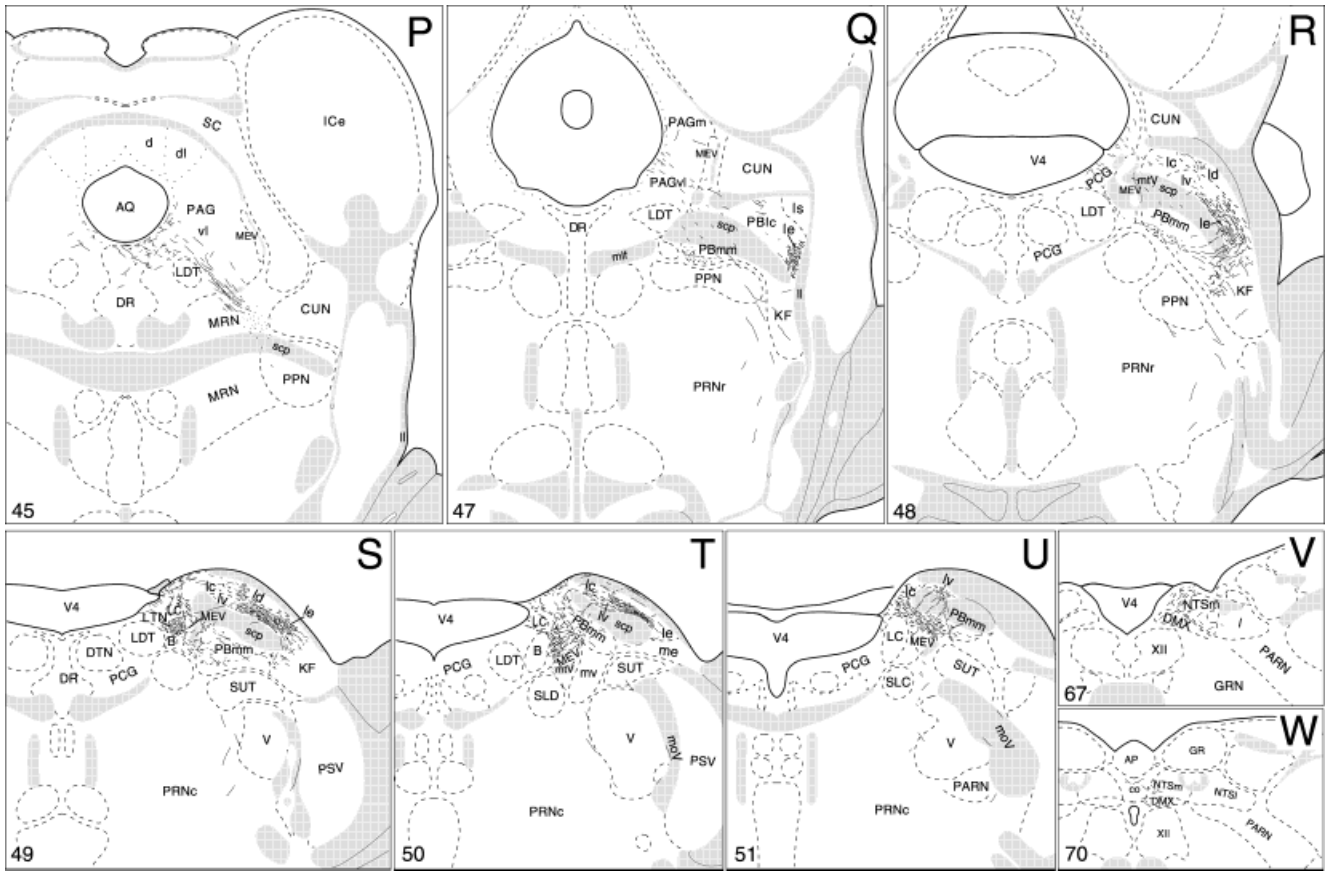

Figure 4 (Continued)

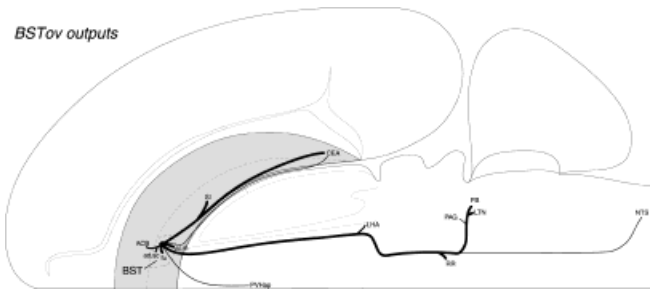

Fig. 5. Summary diagram to indicate the general organization of projections from the BSTov. The relative size of each pathway is roughly proportional to the thickness of the line representing it. The BSTov provides very sparse contralateral projections, which are not shown here. Flat map is based on Swanson (1999).

Most of the BSTov axons descending though the medial forebrain bundle end in the parabrachial nucleus, where there are dense terminal fields in the external lateral, ventral lateral, central lateral, and a restricted region of the dorsal lateral part of the lateral division (Figs. 3C, 4Q–U). In addition, there is a light input to the medial region and a dense input to the caudodorsal ("waist") region of the medial division (Fig. 4Q–U). A few PHAL-labeled axons were also observed in the Kölliker-Fuse subnucleus (Fig. 4R,S).

In addition, there is a dense, obvious terminal field in the lateral tegmental nucleus (Figs. 3C, 4S,T) and a small number of fibers in regions around the rostral locus coeruleus; some of the latter fibers extend laterally into the ependymal lining of the fourth ventricle (Fig. 4S–U). Finally, a small number of PHAL-labeled axons with terminal boutons were found in the medial part of the nucleus of the solitary tract (Fig. 4V,W).

Projections from the BSTfu

The BSTfu, like the BSTov, contains many CRH-expressing neurons. Therefore, the nuclear borders of the BSTfu were also confirmed by CRH mRNA hybridization in experiments involving PHAL injections aimed at it (see Fig. 2A′–C′). In five experiments, the PHAL injection labeled many neurons in the very tiny BSTfu. Three injection sites that were mostly restricted to the BSTfu are shown in Figure 1, although in each case there were a few PHAL-labeled neurons in adjacent areas, especially in the BSTdm and BSTsc and in the parastrial nucleus (Fig. 1, BST44, BST92, BST106). The same pattern of projections was observed in all these experiments, and experiment BST92 was chosen to illustrate in detail because the injection site spreads less from the BSTfu than in the other experiments (Figs. 1, BST92, 2A′–C′). Considering the size and shape of the BSTfu, it is doubtful that a perfect PHAL injection can be obtained, and considering its probable projection pattern it also seems unlikely that it

can ever be completely validated with retrograde tracer methods.

Nevertheless, several PHAL control injections were made in areas surrounding the BSTfu, including the dorsomedial nucleus and subcommissural zone of the BST. These two areas were examined in some detail because they contained a few labeled cells in the experiment to be described in detail (BST92). The projections of the parastrial nucleus, which is adjacent to the BSTfu and which also contained a few PHAL-labeled neurons in the BSTfu experiments, have been described elsewhere (Simerly and Swanson, 1989; Thompson and Swanson, in preparation).

By way of introduction, the BSTfu displays a much more complex pattern of projections than that observed for the BSTov (Figs. 6, 7). Within the BST, the BSTfu projects densely to the caudoventral corner of the anterolateral area, to the anterodorsal area, and to the dorsomedial nucleus; it projects moderately to the oval and rhomboid nuclei and subcommissural zone; and it projects lightly to the rostral anterolateral area and ventral nucleus. Some of the longer projections of the BSTfu are like those of the BSTov in that they ascend into the rostral telencephalon, they course through the stria terminalis and ansa peduncularis to reach the amygdala, and they descend through the medial forebrain bundle to innervate the lateral hypothalamus and lower brainstem nuclei. However, axons from the BSTfu provide a very dense input to the perifornical area of the lateral hypothalamic area, which receives only a very light input from the BSTov, and the BSTfu sends very dense projections to the hypothalamus via periventricular and ventral routes, which is strikingly different from the BSTov.

Local and ascending projections. Within the BST, a group of fibers displaying branches with rich boutons extends *dorsomedially* from the BSTfu through the dorsomedial nucleus and anteroventral area and then arches around the medial edge of the anterior commissure to enter the anterodorsal area (Fig. 6D–F). Fibers with numerous branches and terminal boutons can then be observed in the rostral end and central core of the anterodorsal area (Fig. 6D–F), whereas caudal regions of the anterodorsal area receive only light inputs that appear to arrive via the dorsal route (see next paragraph). Some axons continue dorsally and rostrally throughout the anterodorsal area of the BST to innervate more rostral parts of the telencephalon (see below).

Another group of PHAL-labeled axons from the injection site extends *dorsally* through the subcommissural zone of the BST, where moderate numbers of boutons-of-passage and terminal boutons are seen (Fig. 6G), to provide a moderate input to the caudoventral BSTov and adjacent bordering regions of the anterodorsal area (Figs. 2B′, 6G). Curiously, the rostral BSTov is almost completely avoided by PHAL-labeled axons (Fig. 6F).

PHAL-labeled axons in the anterodorsal area of the BST extend *laterally* into the rostral anterolateral area of the BST, which is only lightly innervated by the BSTfu (Fig. 6E), and they also extend dorsomedially into the lateral septal nucleus, where small numbers of terminal boutons are observed, mainly in the rostral and ventral parts (Fig. 6B–H). Interestingly, most of the PHAL-labeled axons in the anterodorsal area of the BST extend *rostrally* to generate a dense terminal field in the most caudal (dorsomedial) regions of the nucleus accumbens (Fig. 6C). In more rostral levels of the nucleus accumbens, the PHAL-labeling dramatically decreases, and only a small number of axons can be observed medially in the nucleus (Fig. 6A,B). These fibers continue ventrally to provide a light input to the olfactory tubercle, where a small number of terminals were observed in all three layers (Fig. 6B). A few PHAL-labeled axons were also found in the rostroventral substantial innominata (Fig. 6B–H), and even fewer PHAL-labeled axons with terminal boutons could be traced into the infralimbic cortical area (Fig. 6A).

From the BSTfu injection site, large numbers of PHAL-labeled axons also extend *caudally* into the caudoventral corner of the anterolateral area of the BST and the adjacent substantia innominata. Numerous fibers with rich branching and terminal boutons appear to provide dense inputs to these areas (Fig. 6H,I). However, the lateral interfascicular and transverse nuclei of the BST, which are densely innervated by the BSTov, contain only scattered fibers-of-passage (Fig. 6J). The rhomboid and ventral nuclei of the BST contain a moderate plexus of PHAL-labeled axons with rich terminal boutons, whereas the rest of the BST contains only scattered fibers-of-passage (Fig. 6H,I). As we shall now see, the longer, extrinsic projections from the BSTfu were observed to follow five distinct pathways to the amygdala, hypothalamus, and lower brainstem (Figs. 6A–Z, 7).

Ansa peduncularis pathway. As described in the preceding section, many PHAL-labeled fibers from the injection site course through the caudoventral corner of the anterolateral area of the BST to provide a dense input to adjacent caudal dorsolateral regions of the substantia innominata (Figs. 3A′, 6H–J). However, unlike the projection from the BSTov, PHAL-labeled axons from the BSTfu generate many fewer branches and terminal boutons when they travel through more caudal regions of the substantia innominata toward the amygdala (Fig. 6J–M).

Within the amygdala, the CEAm receives a dense terminal field generated by abundant fibers displaying branches and terminal boutons (Figs. 3B′, 6L–O). Very few PHAL-labeled axons with terminal boutons were also found in the CEAc and CEAl (Fig. 6K–O). Finally, the posterior basolateral nucleus and postpiriform transition area also receive light inputs (Fig. 6Q–S), whereas the rest of the amygdala is almost free of PHAL labeling.

Stria terminalis pathway. A bundle of axons from the BSTfu travels dorsally through the anterodorsal area, through the BSTov, and more caudally through the rhomboid nucleus to enter the stria terminalis and travel caudally toward the amygdala (Fig. 6G–P). After entering the amygdala, these axons cannot be distinguished from those arriving via the ansa peduncularis pathway.

Medial forebrain bundle pathway. The BSTfu uses this pathway to send a very dense projection to the lateral hypothalamic area, and moderately dense projections to more caudal sites in the brainstem. From the injection site, labeled axons travel through a circumscribed region that includes the caudal anterolateral area of the BST, caudal dorsomedial regions of the substantia innominata, and adjacent regions of the lateral preoptic area to enter the lateral hypothalamic area (Fig. 6H–L). Compared to descending fibers from the BSTov described above, PHAL-labeled axons arising in the BSTfu travel though more ventromedial regions of the medial forebrain bundle (Fig. 6K–Q). Initially, the fibers in the lateral hypothalamic area are cut in cross-section and generate almost no bou-

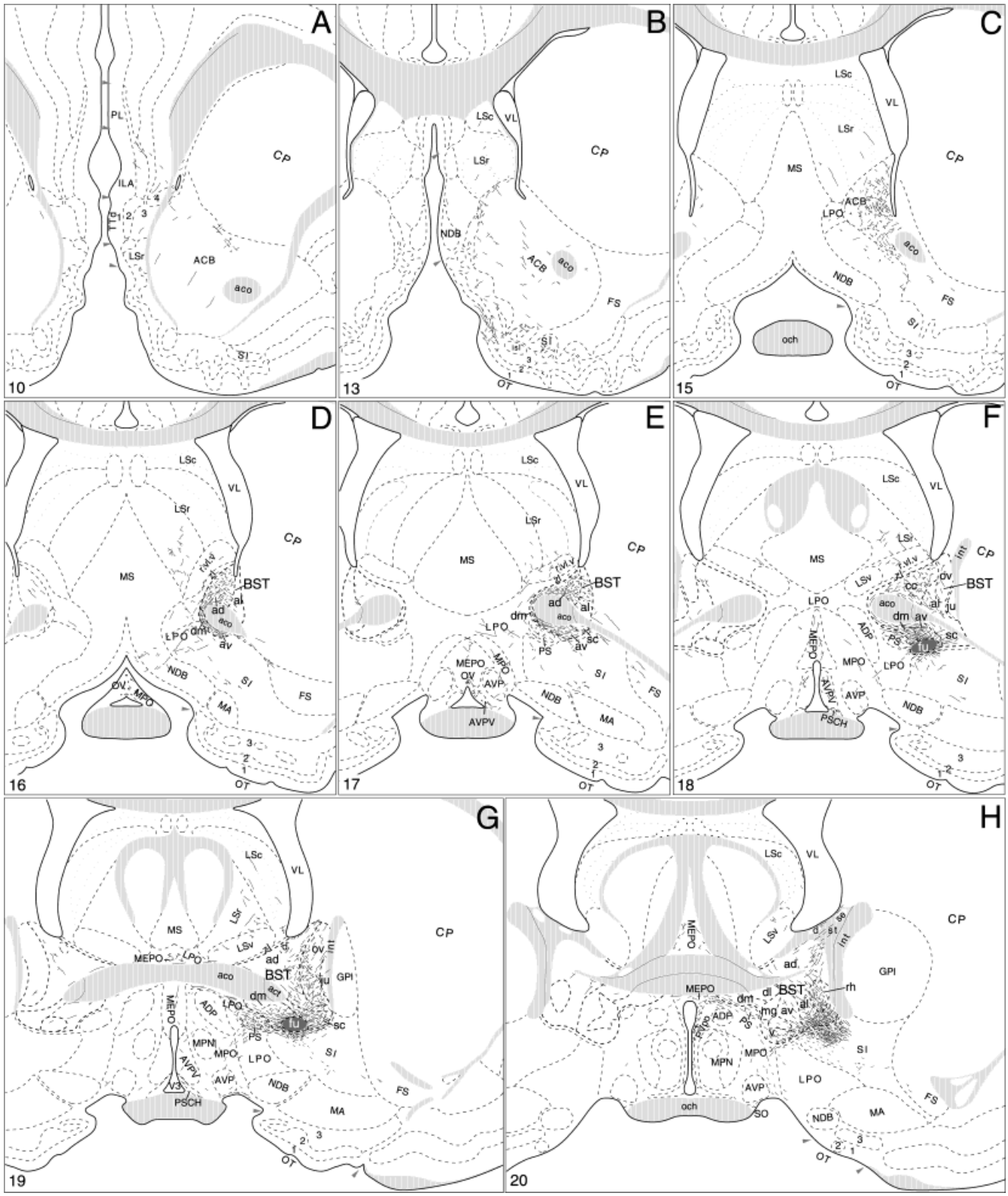

Fig. 6. **A–Z:** Summary of BSTfu projections. The distribution of PHAL-labeled axons in experiment BST92 was plotted onto a series of standard drawings as in Figure 4. The dark gray area in the BSTfu (G) indicates the injection site (see Figs. 1, 2).

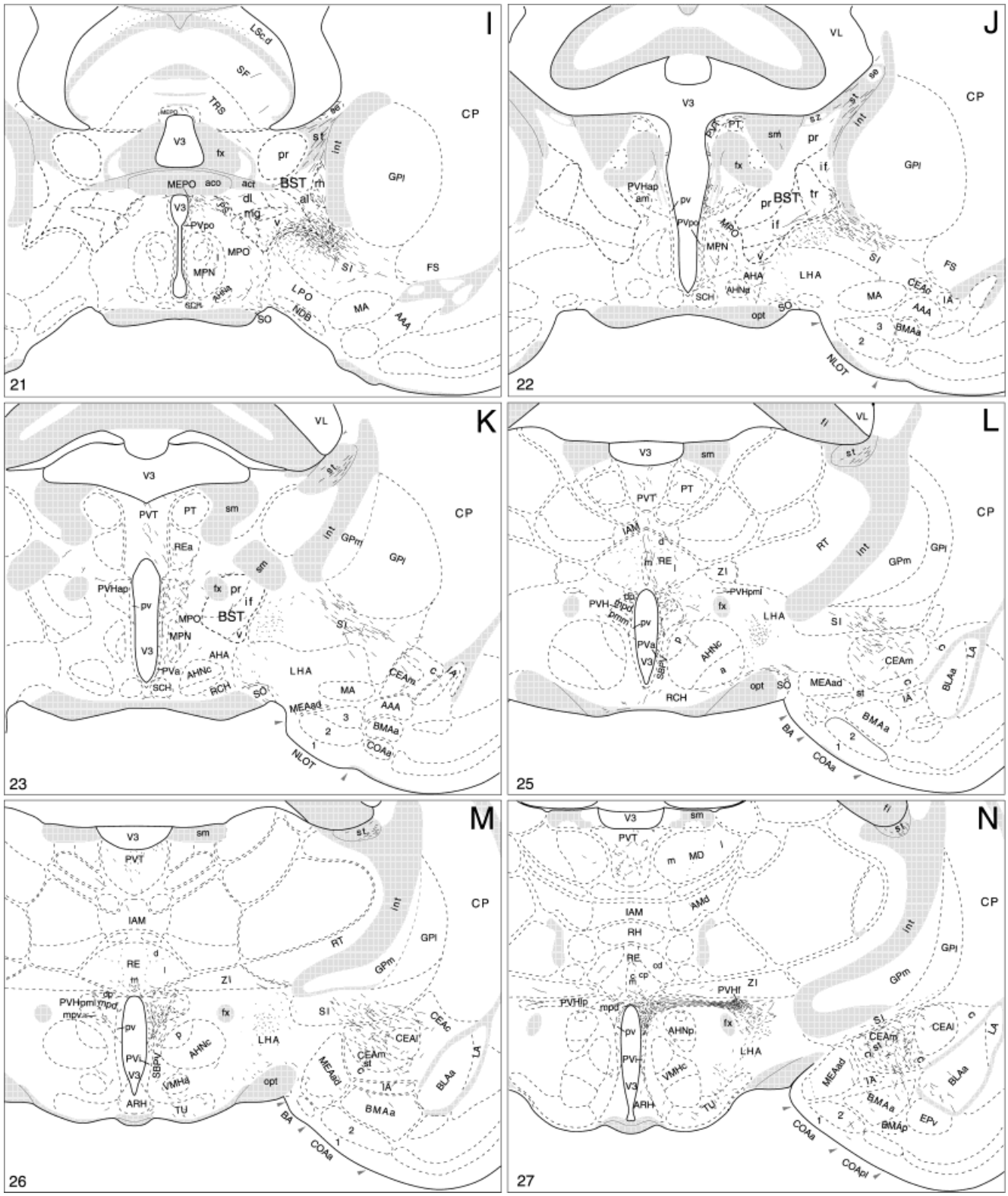

Figure 6 (Continued)

tons until they arrive at tuberal levels (Fig. 6N), where they generate many branches and boutons in an area just dorsolateral to the fornix. This is a dense terminal field in the forniceal part of the paraventricular nucleus (PVH; Figs. 3D′, 6N, 8G′,H′). From this terminal field a group of PHAL-labeled fibers extends medially through the lateral

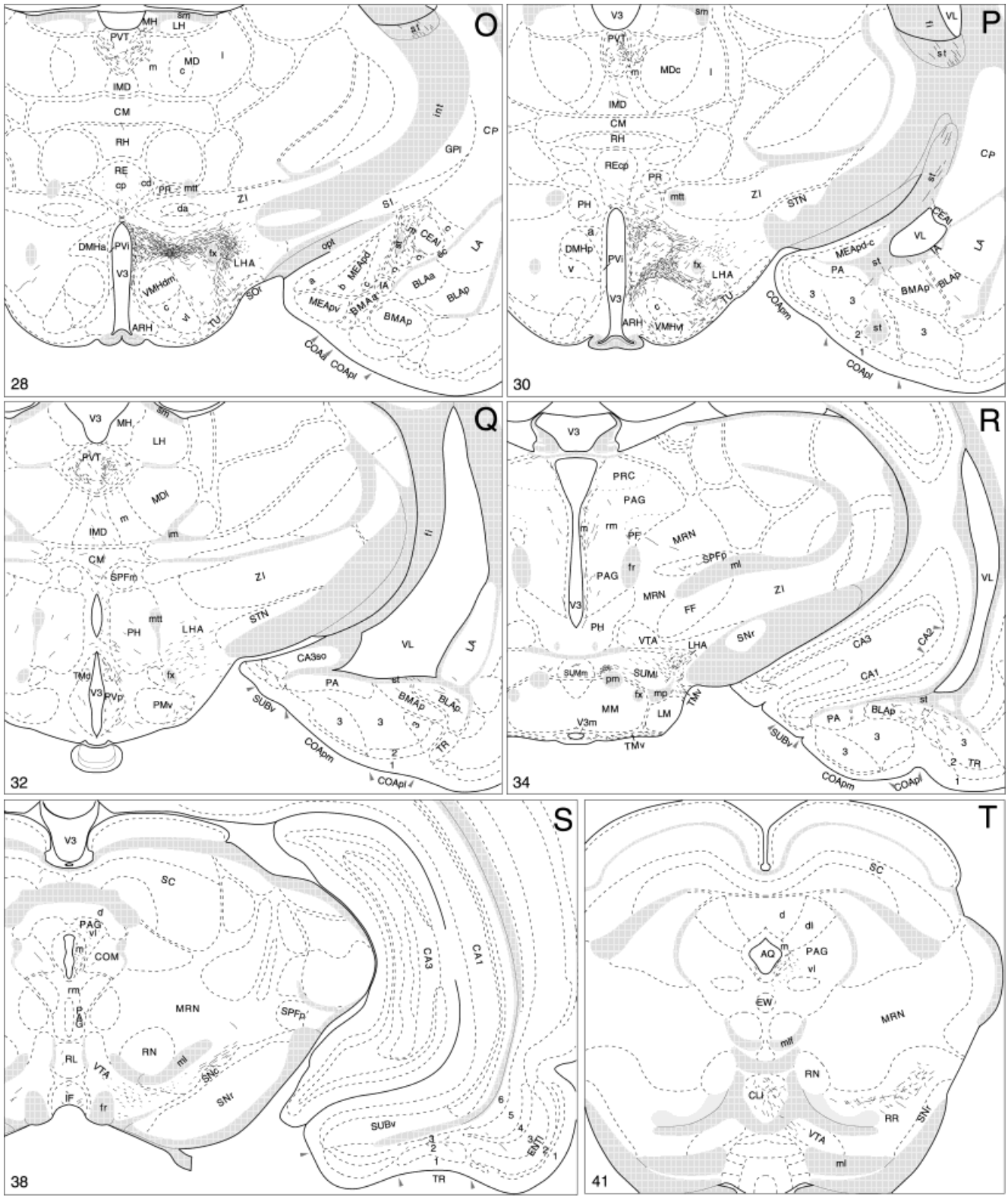

Figure 6 (Continued)

parvicellular part of the PVH, which also contains dense terminal boutons, to contribute inputs to all of the more medial parts of the nucleus, but especially the dorsal medial parvicellular and periventricular parts at atlas (Swanson, 1999) levels 26 and 27 (Figs. 3D, 6M,N, 8G′,H′).

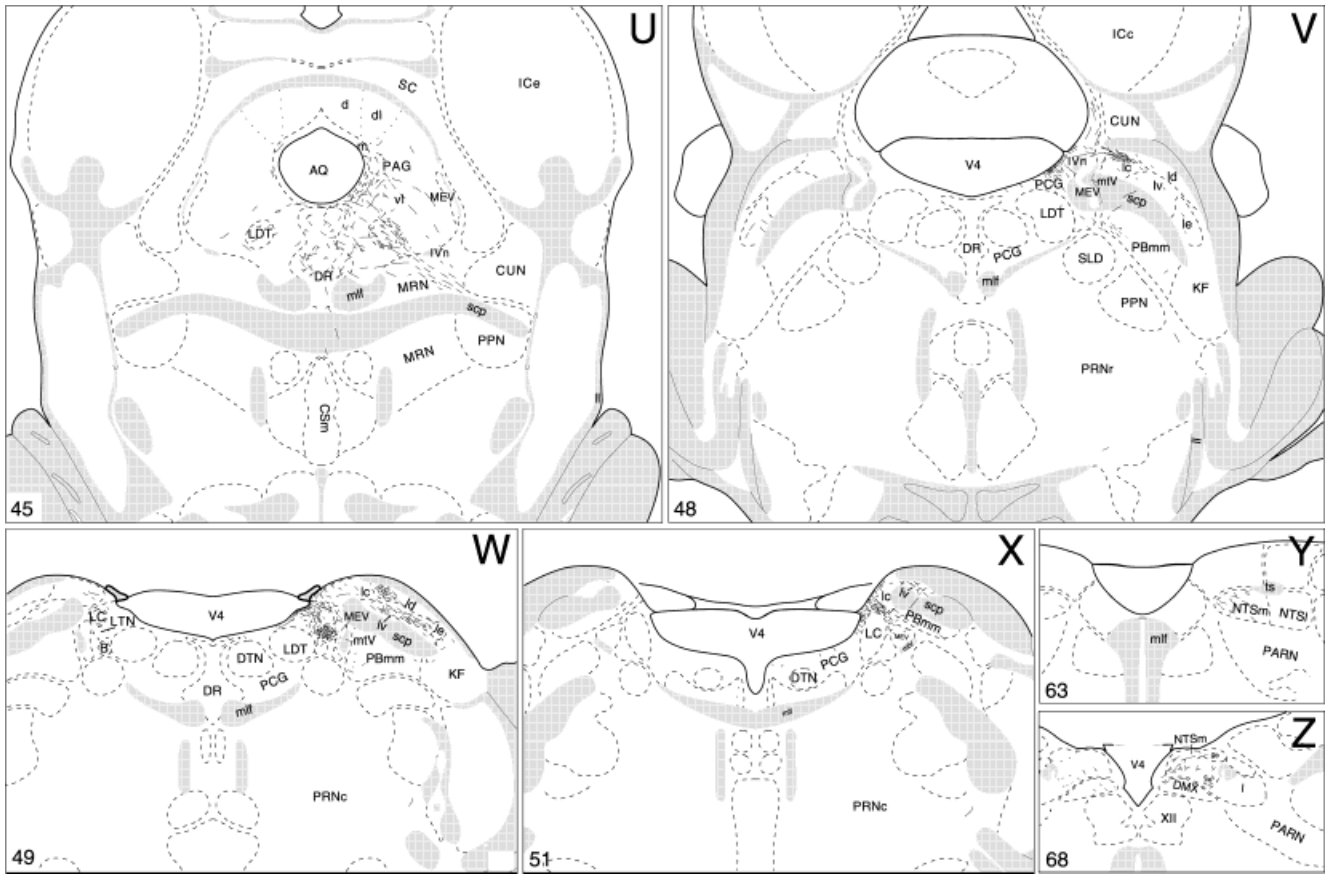

Figure 6 (Continued)

Just caudal to the forniceal part of the PVH, axons from the BSTfu provide a very dense input to a region of the lateral hypothalamic area capping the fornix; numerous branches and terminal boutons were observed here (Figs. 3E′, 6O). This terminal field extends medially into the dorsomedial nucleus of the hypothalamus (Figs. 3E′, 6O), which is heavily innervated by fibers that seem mainly to arrive via the periventricular and ventral pathways (see below).

Interestingly, at levels of the map caudal to P (Fig. 6), labeled fibers, branches, and terminal boutons in perifornical regions of the lateral hypothalamic area decrease dramatically. A small number of PHAL-labeled fibers can be seen extending through the posterior hypothalamic nucleus and contributing inputs to the midline nuclei of the thalamus (Fig. 6P,Q), whereas the remaining PHAL-labeled axons extend caudally. Unlike the BSTov, the BSTfu does not innervate the parasubthalamic nucleus of the lateral hypothalamic area (Fig. 6Q), although a few branches and terminal boutons can be seen in the most caudal region of the lateral hypothalamic area (Fig. 6R). At this level, small numbers of fibers course medially to enter the lateral part of supramammillary nucleus and generate a very distinct terminal field in a small region just dorsomedial to the principal mammillary tract (Fig. 6R). In addition, a few axons can be found in the medial supramammillary nucleus (Fig. 6R).

The remaining PHAL-labeled axons from the BSTfu that travel through the lateral hypothalamic area enter the midbrain, where they course through the ventral tegmental area to reach more caudal brainstem nuclei (Fig. 6R,S). PHAL-labeled axons traveling through the ventral tegmental area display very few branches and boutons (Fig. 6S) and follow median and lateral pathways to reach the pons.

The median pathway. Small numbers of PHAL-labeled axons course medially from the ventral tegmental area though the interfascicular and central linear nuclei of the raphé (Fig. 6S,T) to end in the dorsal nucleus of the raphé (Fig. 6U). Along the way, these fibers generate very few boutons except in the dorsal raphé, where there is a moderate input (Fig. 6U). Some PHAL-labeled axons in the dorsal nucleus of the raphé also extend laterally into the ventrolateral division of the periaqueductal gray, where they merge with fibers arriving from the lateral pathway described next (Fig. 6U).

The lateral pathway. Most PHAL-labeled fibers in the ventral tegmental area travel caudolaterally through an area between the medial lemniscus and substantia nigra (Fig. 6S), then the retrorubral area, and then dorsolateral mesencephalic reticular nucleus, to arrive in the ventrolateral division of the periaqueductal gray (Fig. 6T,U). The BSTfu provides moderate inputs to the retrorubral area (Fig. 6T) and ventrolateral division of the periaqueductal gray (Fig. 6U) and a light input to the rostral laterodorsal tegmental nucleus (Fig. 6U).

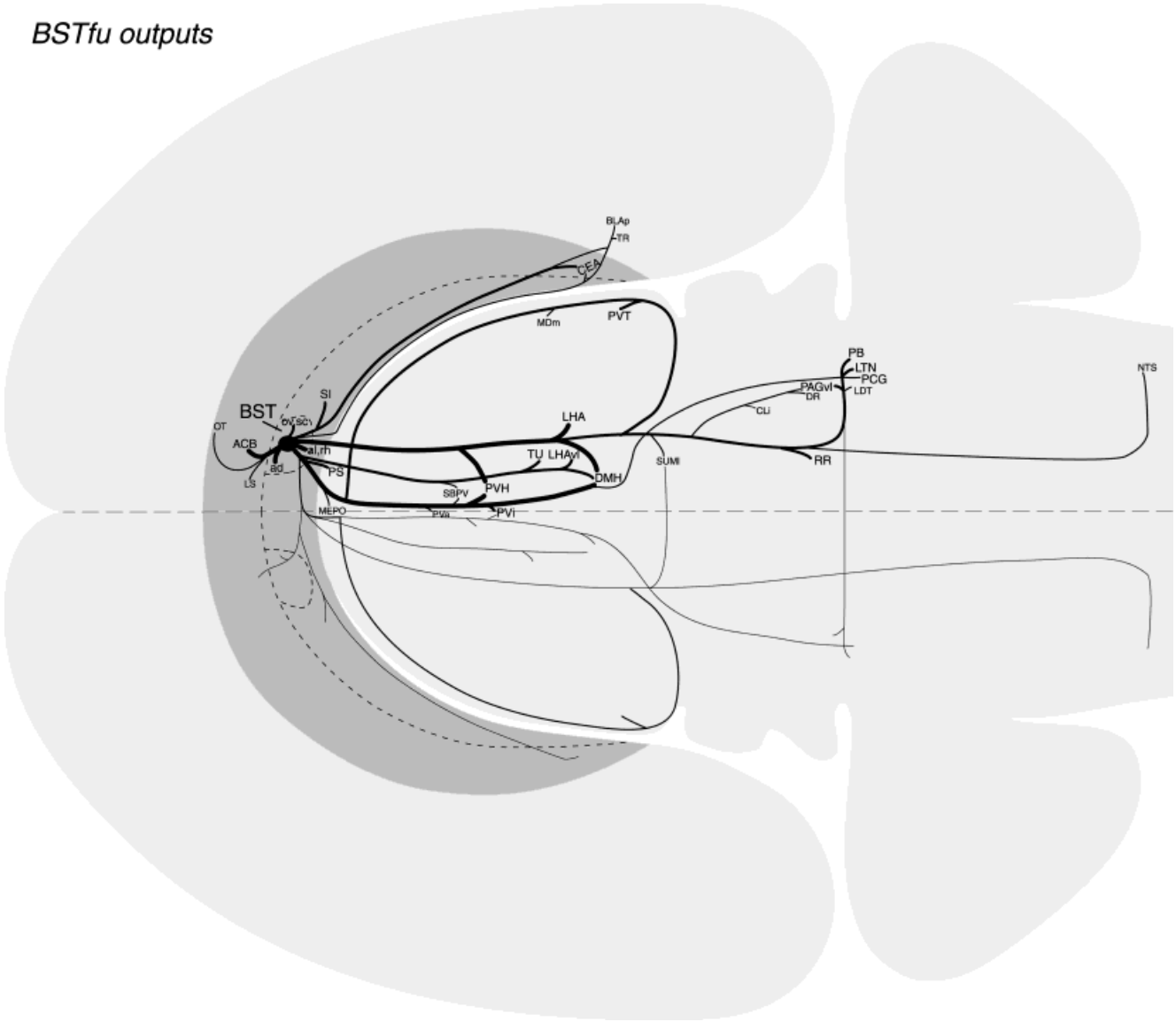

Fig. 7. Summary diagram to indicate the general organization of projections from the BSTfu plotted as in Figure 5.

The BSTfu innervates regions of the parabrachial nucleus different from those innervated by the BSTov. Thus, rostrodorsal regions of the central lateral and dorsal lateral parts, and caudal regions of the ventral lateral and central lateral parts, contain moderate numbers of terminal boutons after BSTfu injections (Figs. 3C′, 6V,W). However, the external lateral part, the most caudal regions of the ventral lateral part of the lateral division, and the medial division (especially the "waist" area)—regions that are heavily innervated by the BSTov—receive only very light projections from the BSTfu (Fig. 6W,X).

In the pontine central gray, the BSTfu, like the BSTov, provides a distinct terminal field in the lateral tegmental nucleus (Figs. 3C′, 6W). Interestingly, numerous fibers were also observed dorsomedially around the rostral end of the locus coeruleus, although very few axons were found within the nucleus itself (Fig. 6W,X). In addition, many fibers extend into the ependymal wall of the fourth ventricle (Figs. 3C′, 6W,X). Finally, a few PHAL-labeled fibers with terminal boutons were observed in the medial part of nucleus of the solitary tract (Fig. 6Y,Z).

The ventral pathway. In the caudal BST, a group of PHAL-labeled axons courses ventromedially through the ventral nucleus of the BST to the medial preoptic area and then turns caudally to run near the ventral surface of the hypothalamus in the vicinity of the supraoptic nucleus (Fig. 6H–J). These fibers generate a few branches and boutons in the retrochiasmatic area, in the area just dorsal to the surface of the supraoptic nucleus (Fig. 6K,L), and in the supraoptic nucleus itself (Fig. 6J–L). Then, more caudally, these axons generate a small number of branches and boutons in the tuberal nucleus (Fig. 6M–P)

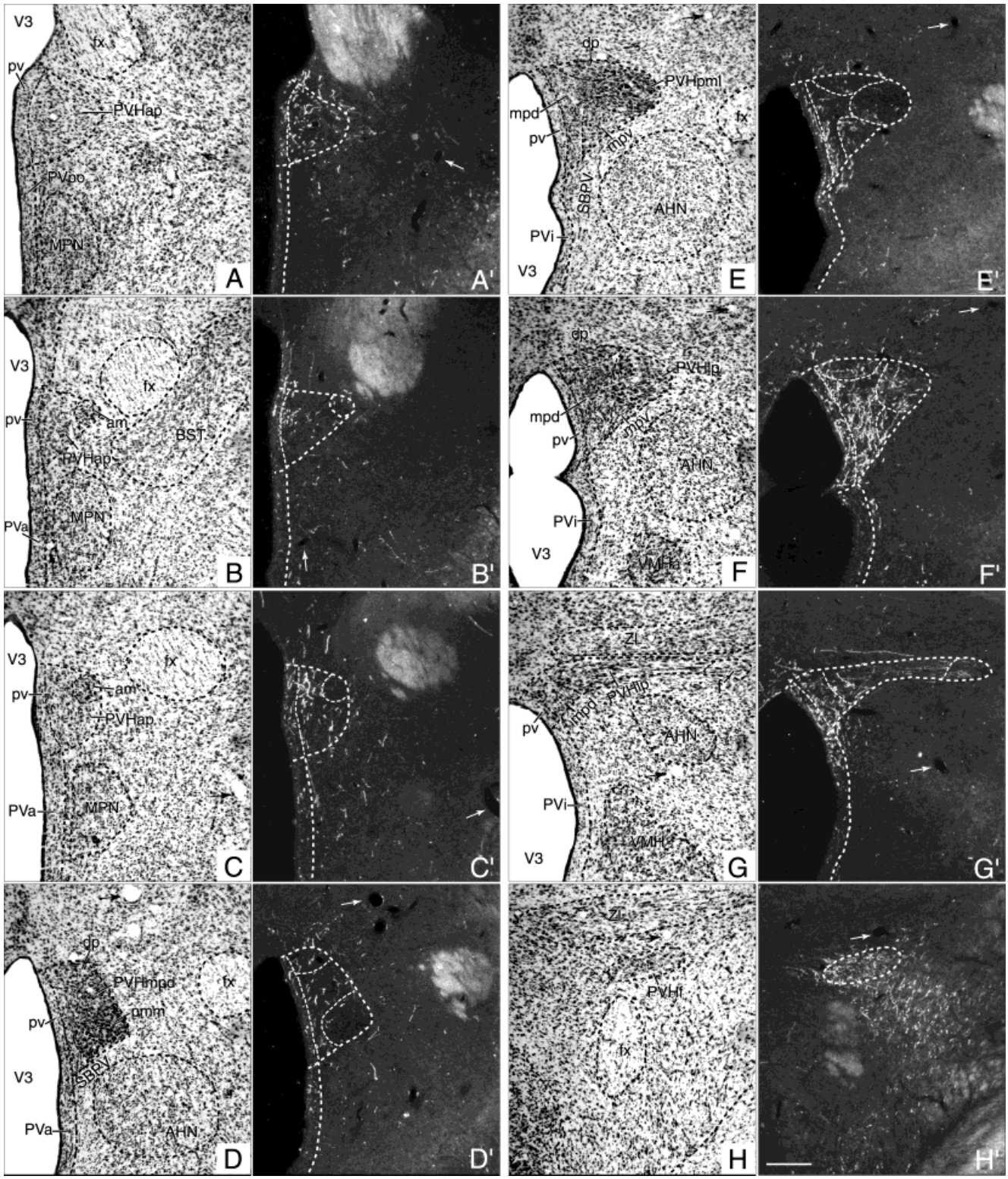

Fig. 8. Darkfield photomicrographs showing the appearance of PHAL-labeled axons from the BSTfu (experiment BST92) in transverse histological sections through the hypothalamic paraventricular nucleus from rostral to caudal (**A′–H′**). For subdivisions of the paraventricular nucleus, see the corresponding caudally adjacent thionin-stained transverse sections (**A–H**). Scale bar = 200 μm.

before turning dorsally and branching profusely in the circumscribed lateral hypothalamic terminal field surrounding the fornix that was described above for the medial forebrain bundle pathway (Fig. 6O,P). Near the rostral end of the dorsomedial nucleus, this plexus of fibers merges with the plexus from the *medial forebrain bundle* lateral to the fornix (Figs. 3E′, 6O), whereas more caudally they turn dorsomedially to join a fiber plexus in the ventral part of the dorsomedial nucleus (Fig. 6P). The *ventral* pathway seems to end as a few scattered axons in and ventral to the ventral premammillary nucleus (Fig. 6Q).

The periventricular pathway. This is a major pathway from the BSTfu to the periventricular zone of the hypothalamus. From the BSTfu, PHAL-labeled axons first course medially through the dorsomedial nucleus of the BST and the parastrial nucleus, which receive moderate terminal fields consisting of branches and terminal boutons. The pathway then crosses the dorsal extreme of the medial preoptic area to enter the periventricular zone, just ventral to the crossing of the anterior commissure (Fig. 6G–I). Some fibers also enter the periventricular zone from a slightly more rostral position (Fig. 6D–F). At preoptic levels, these PHAL-labeled axons display very few terminal boutons in the anteroventral, median preoptic, and preoptic periventricular nuclei (Fig. 6E–J). However, more caudally, this pathway from the BSTfu provides a major terminal field within the PVH.

Different components of the PVH are topographically innervated by PHAL-labeled fibers (Fig. 8). Thus, the anterior parvicellular and adjacent periventricular parts are moderately innervated (Figs. 6J,K, 8A′,B′), whereas the anterior magnocellular part contains only a few PHAL-labeled fibers (Figs. 6J, 8B′,C′). More caudally, the rostral end of the dorsal medial parvicellular and dorsal parvicellular parts, and the posterior magnocellular part, contain only scattered fibers (Figs. 6L, 8D′,E′). However, the PHAL-labeled axons display numerous branches and terminal boutons more caudally in the dorsal medial parvicellular part and adjacent regions of the periventricular part (Figs. 3D′, 6M,N, 8F′,G′). The lateral parvicellular part also contains a dense terminal field (Figs. 3D, 6N, 8F′), whereas the dorsal parvicellular and ventral medial parvicellular parts contain only a small number of PHAL-labeled terminal boutons (Figs. 6M, 8E′,F′). Interestingly, at the most caudal levels of the PVH, many very fine PHAL-labeled axons with numerous branches and terminal boutons were observed to extend laterally through the lateral parvicellular part into the forniceal part (Figs. 3D′, 6N, 8G′,H′). However, the major terminal fields in the forniceal and lateral parvicellular parts of the PVH probably arise, at least in part, from the medial forebrain bundle pathway (see above).

The caudal half of the intermediate part of the periventricular nucleus is heavily innervated by very dense PHAL-labeled fibers with numerous branches and terminal boutons (Figs. 3E′, 6O,P), whereas the rest of the nucleus contains only what appear to be fibers-of-passage. In addition, the arcuate nucleus contains a small number of PHAL-labeled fibers (Fig. 6P).

Most of the remaining axons in the periventricular pathway extend caudally to innervate the dorsomedial nucleus of the hypothalamus, where numerous PHAL-labeled branches with abundant boutons were observed in the anterior and ventral parts (Figs. 3E′, 6O,P). It should be noted that fibers contributing to the terminal field in the dorsomedial nucleus arrive not only from the *periventricular* pathway but also from the *medial forebrain bundle* and *ventral* pathways as well (Fig. 6O,P). Curiously, the posterior division of the dorsomedial nucleus is virtually free of PHAL labeling except for scattered axons (Fig. 6P).

Only a few PHAL-labeled axons with terminal boutons were observed in the posterior periventricular nucleus (Fig. 6Q), and small numbers of fibers extend caudally though the periaqueductal gray (Fig. 6Q,R). Most of the latter travel in the medial and adjacent ventrolateral divisions of the periaqueductal gray to end in the area of pontine central gray near the wall of the fourth ventricle (Fig. 6R–U).

Finally, the BSTfu provides a dense bilateral projection to the caudal paraventricular nucleus of the thalamus via the *periventricular* pathway. The largest group of fibers ascends into the thalamus at rostral levels (Fig. 6K,L), although a few axons-of-passage may be seen to ascend directly to the paraventricular nucleus of the thalamus throughout the length of the midline thalamus (Fig. 6L–Q). These fibers provide dense terminal fields in the caudal paraventricular nucleus and also innervate immediately adjacent regions of the medial mediodorsal nucleus (Fig. 6N–Q). However, there are only a few branches and terminal boutons in the rostral paraventricular nucleus of the thalamus (Fig. 6J–M).

Contralateral projections. Unlike the BSTov, the BSTfu projects lightly to the contralateral side. Most of the crossed projections emerge from the *periventricular* pathway, and they tend to mirror the ipsilateral projection pattern (Fig. 7).

From the injection site, groups of PHAL-labeled fibers cross the midline dorsal and ventral to the anterior commissure to enter the contralateral BST (Fig. 6G–I). Rostrally, a few axons also extend medially through the lateral preoptic area from the ipsilateral BST to enter the contralateral BST (Fig. 6D–F), where most branches and boutons are in the anterodorsal area (Fig. 6D–G). The PHAL-labeled axons emerging from the contralateral BST basically follow the same pathways as described for the ipsilateral projection. Rostrally, they end in the nucleus accumbens (Fig. 6A–C), whereas, caudally, a very few axons course through the substantia innominata (Fig. 6J) to end in the CEAm (not shown here). However, most fibers take the periventricular pathway to innervate the contralateral periventricular and paraventricular nuclei of the hypothalamus (see below).

At all levels of the hypothalamus, scattered fibers from the ipsilateral periventricular pathway cross the midline just dorsal to the third ventricle to enter the contralateral periventricular zone (Fig. 6K–Q). Specifically, these axons travel through ventral regions of the nucleus reuniens to end mainly in the contralateral paraventricular and dorsomedial nuclei (Fig. 6K–P). In addition, a few of these axons also ramify in the contralateral lateral hypothalamic area at the level of the dorsomedial nucleus (Fig. 6O,P). A few axons also cross the midline through the retrochiasmatic area in the supraoptic commissures to end in the contralateral subparaventricular zone and tuberal nucleus (Fig. 6K–N).

Caudally, a small number of axons in the contralateral periventricular pathway course through the posterior hypothalamic nucleus to the contralateral periaqueductal

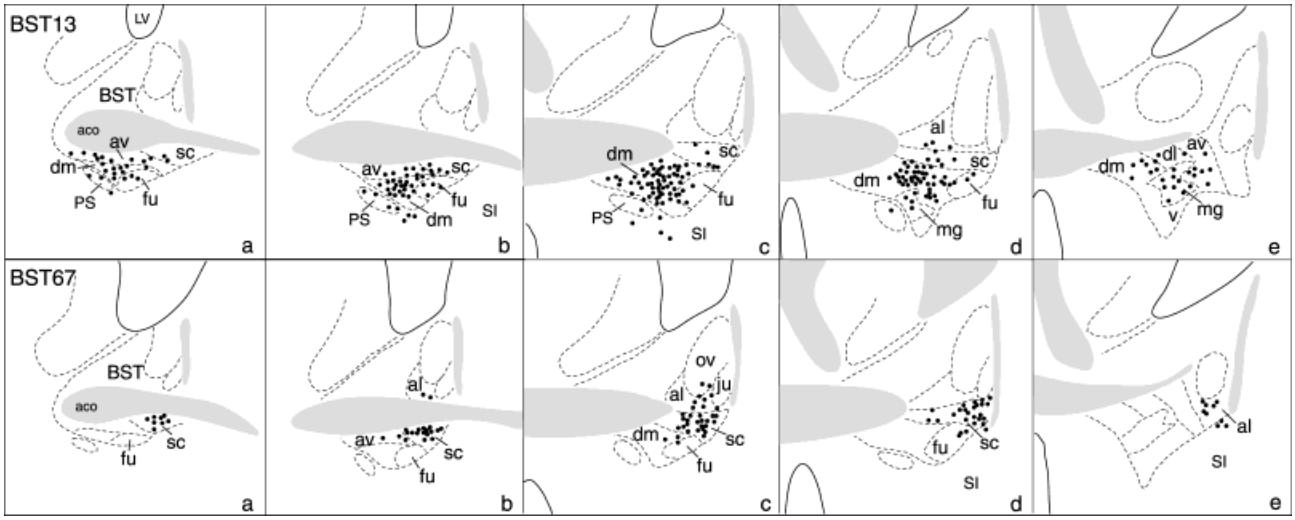

Fig. 9. Camera lucida plots of transverse histological sections with labeled neurons following PHAL injections into the dorsomedial nucleus (experiment BST13) and subcommissural zone (experiment BST67) of the BST, as controls for BSTfu injections (see Fig. 1). In each case, **a–e** is from most rostral to most caudal.

gray (Fig. 6Q–V). A few PHAL-labeled axons were observed in the contralateral parabrachial nucleus and nucleus of the solitary tract (Fig. 6V–Z).

Control injections

It is possible that the very small numbers of labeled neurons outside the BSTfu in the injection sites used here (Fig. 1) contribute to, or actually are responsible for, the very light projections shown in Figure 6. Specifically, the dorsomedial nucleus (BSTdm) and subcommissural zone (BSTsc) of the BST, and the parastrial nucleus, may contribute a few axons to some of the pathways illustrated in Figure 6. To examine this possibility, 15 additional experiments with a PHAL injection centered in these three adjacent areas were analyzed. The projection patterns of the BSTdm and BSTsc will be described fully in a subsequent paper, and the projections of the parastrial nucleus have been described by Simerly and Swanson (1989) and Thompson and Swanson (in preparation). Here we will simply comment on relevant projections as displayed in experiments BST13 (centered in the BSTdm) and BST67 (centered in the BSTsc; Fig. 9).

Projections from the BSTdm (experiment BST13) follow pathways used by the BSTfu to innervate the rostral telencephalon, amygdala, hypothalamus, thalamus, and lower brainstem. The most striking differences between projections of the BSTdm and BSTfu are displayed in the periventricular zone of the hypothalamus. It would appear that terminal fields generated by the BSTdm and BSTfu are located in different, by and large complementary, parts of the PVH. Axons from the BSTdm preferentially target rostral levels of the dorsal medial parvicellular part, whereas more caudal levels are heavily innervated by the BSTfu (Fig. 8F). Furthermore, the BSTdm innervates moderately to heavily magnocellular parts of the PVH, as well as the supraoptic, arcuate, and posterior periventricular nuclei, which receive only scattered PHAL-labeled fibers from injection sites centered in the BSTfu. The BSTdm also provides moderate to dense inputs to caudal regions of the medial preoptic nucleus, which contains very few PHAL-labeled axons in our experiments with injections centered in the BSTfu. Finally, the BSTdm does not project significantly to the parabrachial nucleus, which is moderately innervated by the BSTfu.

The parastrial nucleus does not project significantly to the amygdala, although it provides a very dense input to the periventricular zone of the hypothalamus, including the anteroventral preoptic nucleus, median preoptic nucleus, magnocellular division of the PVH, and supraoptic nucleus, all of which receive only scattered axons from injections centered in the BSTfu. In contrast, the BSTsc does not provide significant projections to the periventricular zone of the hypothalamus, but, like the BSTfu, it does send dense inputs to the CEA and lateral hypothalamic area and a moderate input to the parabrachial nucleus. However, at least in the parabrachial nucleus, its terminal distribution is distinct from that arising in the BSTfu.

In summary, it is possible that these three adjacent regions contribute a few of the labeled axons shown in Figure 6. A detailed analysis with retrograde tracers might clarify this ambiguity. On the other hand, it is clear that the vast majority of labeling, and certainly all of the moderately to densely labeled terminal fields, arise in the BSTfu itself.

DISCUSSION

Our results demonstrate that the BSTov and BSTfu have different though partly overlapping projections to specific regions of the cerebral hemispheres and brainstem (Figs. 5, 7). After briefly reviewing the earlier anatomical literature on these projections, we will consider evidence suggesting that the BSTov and BSTfu, along with the CEA, form a highly interconnected network that

is activated by certain forms of stress but not others. Then, we will review the possible functional significance of projection patterns identified here from the BSTov and BSTfu. Finally, we will consider what is known about afferent regulation of the BSTov and BSTfu, beginning with the highly organized input from the CEA and ending with the expression of nuclear receptors for circulating steroid hormones.

Previous anatomical literature

There is very little corroboration of our results in the literature simply because the precise regions of the BSTov and BSTfu were rarely identified in earlier work. The following has been reported concerning BSTov projections. (1) Retrograde labeling in the "lateral part of the BST" (which includes the BSTov) was found after wheat germ agglutinin-horseradish peroxidase (WGA-HRP) injections in the "dorsal" substantia innominata (Grove, 1988). (2) Retrograde labeling in the nucleus was reported after HRP injections in the CEA (Sun and Cassell, 1993). (3) Fluorogold injections in the caudal nucleus accumbens retrogradely label neurons in all subdivisions of the BST, including the BSTov (Brog et al., 1993). (4) Retrograde tracer injected into the region of the parasubthalamic nucleus retrogradely labels neurons in the BSTov (Grittic et al., 1994). (5) Cholera toxin B injection in the retrorubral area yields dense retrograde labeling in the "lateral part of the BST," which probably includes the BSTov and BSTfu (Berendse et al., 1992). (6) Retrograde tracer evidence indicates that the BSTov projects to the external lateral part and "waist" area of the parabrachial nucleus (Moga et al., 1989, 1990; Sun et al., 1994) and that at least some of these fibers contain CRH, neurotensin, and somatostatin (Moga et al., 1985, 1989). (7) After retrograde tracer injection in the periaqueductal gray, Gray and Magnuson (1992) reported labeled CRH- and neurotensin-immunoreactive neurons in the "dorsal lateral BST." (8) HRP injections in the nucleus of the solitary tract retrogradely label a few neurons in the "dorsolateral part of the BST," which includes the BSTov (Schwaber et al., 1982). Most BST projections to the nucleus of the solitary tract arise in the rhomboid nucleus of the BST (Schwaber et al., 1982; Dong et al., 1999).

The following evidence relevant to BSTfu projections has been reported. (1) Caudal nucleus accumbens fluorogold injections retrogradely label neurons in all subdivisions of the BST, including the BSTfu (Brog et al., 1993). Furthermore, dense anterograde labeling was observed in the caudal nucleus accumbens after cholera toxin B injections into the "ventrolateral" BST (which corresponds to our BSTfu; Georges and Aston-Jones, 2000). (2) Grove (1988) reported retrograde labeling in the general vicinity of the BSTfu after tracer injections in the substantia innominata. (3) Fluorogold injections in the dorsolateral perifornical region of the lateral hypothalamic area, just caudal to the PVH, retrogradely label many neurons in the BSTfu (Kelly and Watts, 1996). (4) Retrograde tracer experiments also indicate that neurons in or near the BSTfu project to the dorsal raphé (Peyron et al., 1998), ventrolateral periaqueductal gray (Gray and Magnuson, 1992), and laterodorsal tegmental nucleus (Satoh and Fibiger, 1986). (5) Moga and colleagues (1989, 1990) used anterograde and retrograde tracer methods to demonstrate a projection from the "ventral lateral subnucleus of the BST" (which includes our BSTfu) to specific parts of the parabrachial nucleus. (6) A projection from the "ventral part" of the BST to the "peri-locus coeruleus region" has been reported with retrograde tracing (Luppi et al., 1995; Lechner and Valentino, 1999). (7) In terms of the diencephalon, retrograde tracer experiments indicate that the BSTfu projects to the PVH (Sawchenko and Swanson, 1983), dorsomedial nucleus (Thompson and Swanson, 1998), and thalamic paraventricular nucleus (Cornwall and Phillipson, 1988; Chen and Su, 1990). Furthermore, it has been shown that CRH neurons in the BSTfu project to the PVH (Moga and Saper, 1994).

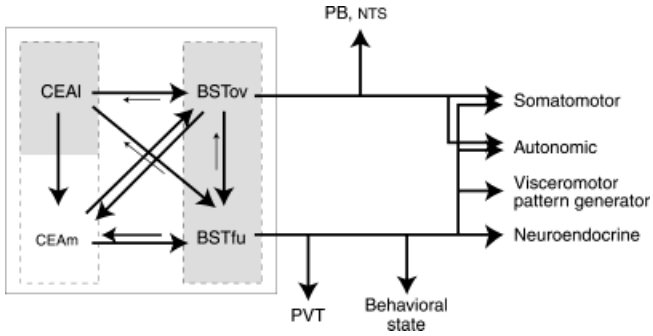

Fig. 10. Summary of connections between the CEAl and CEAm and the BSTov and BSTfu—and of the major outputs of the BSTov and BSTfu—in the rat. First, note that the four cell groups are almost completely interconnected; all that seems to be missing is a projection from the CEAm to the CEAl. However, it is important to note that the relative strength of connections within this network can vary from strong to weak, as indicated qualitatively by line thickness and length. All of these interconnections appear to use GABA as a neurotransmitter; the cell groups highlighted in gray also appear to utilize the neuropeptide CRH. As discussed and documented in the text, descending projections from the BSTov and BSTfu differentially innervate various components of the somatomotor, autonomic, and neuroendocrine motor systems; parts of the brain involved in controlling behavioral state; cell groups that relay viscerosensory and nociceptive information (PB and NTS); and the paraventricular thalamic nucleus (PVT).

Central amygdalar input and functional activation

The organization and significance of BSTov and BSTfu outputs is more readily appreciated if the relationship of these two nuclei with the CEA, and especially with its lateral part, is discussed first. As documented in the introductory paragraphs, many neurons in the BSTov, BSTfu, and CEAl are GABAergic and also express CRH mRNA, and the CEAl sends a dense and rather selective projection to the BSTov and BSTfu. Furthermore, the present results indicate that the BSTov sends a dense projection to the BSTfu and projects to virtually all parts of the CEA, and the BSTfu projects lightly to the BSTov and more heavily to the central amygdalar nucleus (especially the CEAm). Thus, the CEAl, BSTov, and BSTfu share the expression of certain neurotransmitters in common and are massively interconnected (Fig. 10). Furthermore, the CEAm also projects heavily to both the BSTov and the BSTfu (for review see Dong et al., 2001), and, as we have shown here, both of the latter nuclei project to all parts of the CEA. Thus, as outlined in Figure 10, there are bidirectional, probably GABAergic, projections between the CEAm, CEAl, BSTov, and BSTfu. To make the situa-

tion even more complex, there is anatomical evidence for bidirectional, presumably GABAergic, connections between all four cell groups and the capsular part of the CEA as well (see Dong et al., 2001; present results). In short, there is an exceptionally rich network of GABAergic connections involving the various parts of the CEA and the oval and fusiform nuclei of the BST.

It should be noted that the CEAl and BSTov express a much richer set of neuropeptide genes—including at least CRH, neurotensin, somatostatin, enkephalin, and dynorphin (Fallon and Leslie, 1986; Ju and Han, 1989; Ju et al., 1989; Moga et al., 1989; Day et al., 1999)—than other parts of the amygdala and BST. In contrast, CRH is the predominant known peptide expressed in the BSTfu (Ju et al., 1989). These peptides reportedly are always colocalized with GABA or its synthetic enzyme (Oertel et al., 1983; Veinante et al., 1997; Day et al., 1999), although there appear to be at least two distinct GABAergic populations in both the CEAl and the BSTov, one expressing predominantly CRH and neurotensin and the other expressing predominantly enkephalin (Day et al., 1999). In addition, the former GABAergic populations appear to innervate brainstem regions including the central gray, parabrachial nucleus, and dorsal vagal complex, whereas the latter do not (Veening et al., 1984; Moga and Gray, 1985; Gray and Magnuson, 1987; Moga et al., 1989, 1990; Gray and Magnuson, 1992). Furthermore, there is experimental evidence to suggest that projections from the amygdala to the general region of the BSTov contain at least GABA, enkephalin, and neurotensin (Uhl and Snyder, 1979; Ben-Ari, 1981; Palkovits et al., 1981; Rao et al., 1987). Obviously, a great deal remains to be learned about the various classes of neurons (cell types) in the BSTov and BSTfu.

Several experimental models of stress lead to coordinated activation of the CEAl, BSTov, and BSTfu as indicated by increased Fos levels. Stimuli reported thus far include hypertonic saline (Senba and Ueyama, 1997), sodium depletion (Johnson et al., 1999), and angiotensin II, all of which are dipsogenic (Herbert et al., 1992; Rowland et al., 1994), and peripheral administration of interleukin-1 (Brady et al., 1994; Ericsson et al., 1994; Day and Akil, 1996; Day et al., 1999), which is anorexigenic. Levels of Fos are also up-regulated in the CEAl and BSTov (at least) by systemic injections of several other well-known anorexigenic agents, including bombesin, cholecystokinin, satietin, and dexfenfluramine (Bonaz et al., 1993; Li et al., 1994; Li and Rowland 1995; Rowland et al., 1996); by peripheral administration of the immune activator lipopolysaccharide (LPS; Lacroix and Rivest, 1997), which is anorexigenic; and by intracerebroventricular injections of CRH (Bittencourt and Sawchenko, 2000; Chan et al., 2000) and the related peptide urocortin (Bittencourt and Sawchenko, 2000), which are also anorexigenic. Furthermore, it has been shown that levels of CRH neuropeptide mRNA are also clearly altered in the CEAl, BSTov, and BSTfu after dehydration and food restriction (Watts et al., 1995; Watts, 2000, 2001) and that corticosterone itself can, to a greater or lesser extent, alter CRH mRNA levels in these three cell groups (Makino et al., 1994; Watts et al., 1995; Watts and Sanchez-Watts, 1995). Finally, it has been reported (Thrivikraman et al., 2000) that Fos levels increase in the CEAl and BSTov after hemorrhage (20% estimated blood volume).

On the other hand, Fos levels in the CEAl, BSTov, and BSTfu do not appear to be altered substantially under certain other experimental conditions, including restraint stress (Bowers et al., 1998), swim stress (Cullinan et al., 1995), and audiogenic stress (Campeau and Watson, 1997). Mechanisms responsible for changing Fos levels in this circuitry remain to be elucidated. Presumably, they are mediated by neural and/or hormonal inputs to the cell groups, which will be reviewed after a brief consideration of how neural projections from the BSTov and BSTfu are organized.

Functional organization of BSTov and BSTfu projections

Obviously, these two nuclei have multiple and diverse projection fields as defined anatomically, and their functional significance remains to be determined experimentally. Nevertheless, it would appear from a qualitative perspective that most of the terminal fields seem to be associated with four components of the motor system, with the behavioral state system, and with visceroceptive/nociceptive systems (Fig. 10).

The four influences on the motor system broadly conceived include the following. First, both the BSTov and the BSTfu project to at least three regions that are thought to modulate somatomotor responses: the nucleus accumbens, substantia innominata, and retrorubral field. Although the functional significance of these ventral striatopallidal-associated regions is far from clear, there is good evidence that they are at least involved in modulating locomotor, orofacial, and perhaps ingestive behaviors (Swanson et al., 1984; Mogenson et al., 1985; Von Krosigk and Smith, 1990; Spooren et al., 1993; Stratford and Kelley, 1999; Swanson and Kalivas, 2000). Second, both the BSTov and the BSTfu project to four regions involved in controlling the output of the autonomic nervous system: the central nucleus of the amygdala, the dorsal regions of the tuberal lateral hypothalamic area, the parabrachial nucleus, and the nucleus of the solitary tract (Loewy, 1991). In addition, the BSTfu projects heavily to the descending division of the hypothalamic paraventricular nucleus, which provides extensive inputs to preganglionic sympathetic and parasympathetic neurons in the brainstem and spinal cord (for review see Swanson, 1987). Third, the BSTfu projects to two nuclei dominated by neuroendocrine motoneurons: the paraventricular and anterior periventricular nuclei of the hypothalamus (Markakis and Swanson, 1997). Thus, the BSTfu is a part of the BST as a whole that is in a position to modulate adrenocorticotropic hormone (ACTH) release (Beaulieu et al., 1986; Dunn, 1987; Roozendadal et al., 1991; Gray et al., 1993), by innervating the region containing neuroendocrine CRH motoneurons in the paraventricular nucleus, and to modulate growth hormone release by innervating neuroendocrine somatostatin neurons in the anterior periventricular nucleus (see Markakis and Swanson, 1997). Indeed, ibotenic acid lesions of the lateral BST that include the BSTov and BSTfu significantly decrease CRH mRNA levels in the medial parvicellular part of the PVH (Herman et al., 1994). Fourth, the BSTfu also projects to multiple components of the recently identified visceromotor pattern generator network in the periventricular region of the hypothalamus, a network that innervates various combinations of neuroendocrine motoneuron pools and pools of preautonomic neurons in the paraventricular nucleus (Ri-

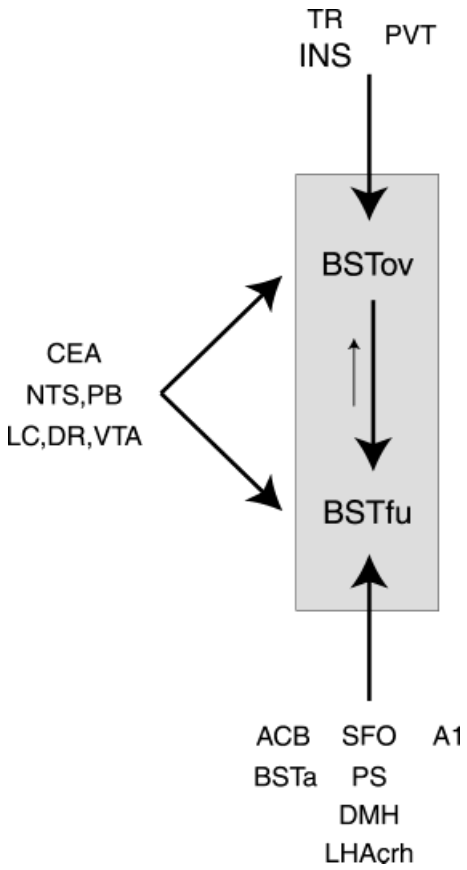

Fig. 11. Summary of major known projections to the BSTov and BSTfu in the rat. These neural pathways are discussed and documented in the text. Note that certain regions of the brain innervate both the BSTov and the BSTfu, whereas there are also differential inputs to each cell group.

sold et al., 1997; Thompson and Swanson, 1998; Swanson, 2000). These nuclei include the dorsomedial, parastrial, and median preoptic nuclei, which are thought to play an especially important role in body water homeostasis (Swanson, 2000).

The BSTfu also projects to three cell groups that may have important influences on behavioral state. Two of them, the dorsal nucleus of the raphé and the laterodorsal tegmental nucleus are centered in the midbrain periaqueductal gray and are thought to regulate various aspects of arousal (Satoh and Fibiger, 1986; Steriade et al., 1990; Vertes, 1990a,b). In contrast, the subparaventricular zone of the hypothalamus receives most of the output of the nearby suprachiasmatic nucleus and thus presumably has an important influence on circadian functions (Watts et al., 1987; Morin et al., 1994).

Finally, both the BSTov and the BSTfu project to the nucleus of the solitary tract and especially the parabrachial nucleus. As mentioned above, these nuclei undoubtedly influence profoundly the output of the autonomic nervous system. However, it is also clear that both nuclei are involved in relaying visceroceptive as well as nociceptive information to more rostral levels of the neuraxis (Ricardo and Koh, 1978; Saper and Loewy, 1980; Bernard et al., 1989, 1993, 1994, 1995; Herbert et al., 1990; Alden et al., 1994; Bester et al., 1997a,b). Therefore, it seems reasonable to suggest that the BSTov and BSTfu may also "gate" the flow of such information to the midbrain and forebrain.

Afferent control of the BSTov and BSTfu

To place the axonal connections of the BSTov and BSTfu described here within a functional context, it may be useful to review briefly what little is known about neural and hormonal inputs to them. To begin with, it is convenient to divide neural inputs into those ending in both cell groups, those ending predominantly in the BSTov, and those ending predominantly in the BSTfu (Fig. 11). As pointed out above (see Fig. 10), both nuclei receive a highly differentiated input from the CEA, which in turn receives virtually all classes of sensory information via a complex set of cortical and subcortical connections (McDonald, 1998; Swanson and Petrovich, 1998). In addition, both nuclei receive inputs from the nucleus of the solitary tract, part of which may be noradrenergic (Ricardo and Koh, 1978; Riche et al., 1990; Terenzi and Ingram, 1995; Georges and Aston-Jones, 2000), and from the parabrachial nucleus, although the lateral parabrachial nucleus tends to innervate both cell groups (Alden et al., 1994), whereas the medial parabrachial nucleus, which preferentially deals with gustatory information, tends to innervate the BSTfu (Herbert et al., 1990; Alden et al., 1994). Whether these pathways from the nucleus of the solitary tract and parabrachial nucleus supply visceroceptive, nociceptive, and/or gustatory information to the BSTov and BSTfu remains to be determined physiologically. Finally, both nuclei appear to receive noradrenergic inputs from the A2 cell group in the nucleus of the solitary tract and A6 cell group in the locus coeruleus (Pickel et al., 1974; Jones and Yang, 1985; Phelix et al., 1992a,b; Aston-Jones et al., 1999; Delfs et al., 2000; Georges and Aston-Jones, 2000), serotonergic inputs from the dorsal nucleus of the raphé (Eiden et al., 1985; Vertes, 1991), and presumably dopaminergic inputs from the ventral tegmental area (Moore, 1978; Hökfelt et al., 1980; Phelix et al., 1992b; Freedman and Cassell, 1994; Risold and Swanson, 1997; Georges and Aston-Jones, 2000).

In contrast, the BSTov also receives inputs from (1) the postpiriform transition area (McDonald, 1998; Dong et al., 2001), a cortical area that receives a massive input from the main olfactory bulb and also projects massively to the CEA (McDonald, 1998; Swanson and Petrovich, 1998); (2) the insular region (Saper, 1982; Yasui et al., 1991; McDonald et al., 1999), which includes visceral, gustatory, and visceroolfactory association areas of cortex; and (3) the paraventricular nucleus of the thalamus (Moga et al., 1995), which receives inputs from many parts of the hypothalamus, including the suprachiasmatic nucleus, and from more caudal regions of the brainstem (for review see Risold et al., 1997).

The BSTfu also receives inputs from several other sites. First, it receives substantial inputs from the anterior division of the BST (H.-W.D. and L.W.S., unpublished observations with PHAL), which is important because the anterior BST receives inputs from the ventral subicular complex of the hippocampus and virtually the entire amygdala (Canteras and Swanson, 1992; for review see Dong et al., 2001). Second, it receives projections from the nucleus accumbens (Groenewegen and Russchen, 1984; Georges and Aston-Jones, 2000), which in turn receives

widespread cortical and subcortical inputs (Groenewegen et al., 1999). Third, it receives inputs from a group of nuclei that have been implicated in the regulation of ingestive behavior, especially in the regulation of thirst (for review see Swanson, 2000). They include the subfornical organ (Swanson and Lind, 1986), parastrial nucleus (R.H. Thompson and L.W.S., unpublished observations with PHAL), dorsomedial nucleus of the hypothalamus (Thompson et al., 1996), and a region of the dorsal tuberal level of the lateral hypothalamic area whose neurons upregulate the expression of CRH when animals experience dehydration (Kelly and Watts, 1996). Fourth, the BSTfu appears to receive an input from the A1 noradrenergic cell group located in the lateral paragigantocellular reticular nucleus of the ventrolateral medulla (Woulfe et al., 1988; Roder and Ciriello, 1994; Zagon et al., 1994; Aston-Jones et al., 1999; Delfs et al., 2000). This pathway appears to be involved in transmitting information received from the nucleus of the solitary tract (Ross et al., 1985).

As mentioned earlier, there is good evidence that adrenal glucocorticoids may influence to varying degrees neuropeptide gene expression in the BSTov and BSTfu, and it should be noted that neurons in both cell groups also express high levels of the androgen but not the estrogen receptor (Simerly et al., 1990) and that neurons in the BSTov also express moderate levels of the mineralocorticoid receptor (Arriza et al., 1988).

OVERVIEW

The results of the present experiments, together with a rather large body of published evidence, suggest at least the outlines of a highly interconnected neural network—consisting of the CEA, BSTov, and BSTfu—that plays an important role in coordinating somatic, autonomic, and neuroendocrine motor responses that attempt to maintain homeostasis in the face of water and/or food deficits. It has recently been suggested that this network is a specialized component of the basal ganglia, cerebral nuclei, or striatopallidum (Swanson and Petrovich, 1998; Swanson, 2000). Thus, the CEA may correspond to a (caudal) part of the striatum, with a defined set of cortical inputs and a dual descending GABAergic projection to the (rostral) pallidum and to a variety of motor system components. The rostral pallidum includes the BSTov and BSTfu, which in turn also send descending GABAergic projections to a variety of motor system components and to the thalamus (Fig. 10).

Adrenal steroid hormones (both glucocorticoids and mineralocorticoids) are critically important for glucose and body water homeostasis, and recent evidence suggests that circulating corticosterone levels, at least, change neuropeptide gene expression in very specific ways after dehydration and/or decreased food intake within neurons of the CEA, BSTov, and BSTfu (for review see Watts, 2000, 2001). It has been proposed that altered neuropeptide levels could, under at least some conditions, alter the physiological effectiveness or strength of projections from these nuclei to sensory and/or motor regions such as the parabrachial and hypothalamic paraventricular nuclei (Watts, 2001). It has also been suggested that conditioned neuropeptide mRNA level changes in the CEAl might act as a reversible "gain control" for long-term modulation of subsequent conditioned responses mediated through the CEAm, BSTov, and/or BSTfu (Petrovich et al., 2000).

LITERATURE CITED

Alden M, Besson, JM, Bernard J-F. 1994. Organization of the efferent projections from the pontine parabrachial area to the bed nucleus of the stria terminalis and neighboring regions: a PHA-L study in the rat. J Comp Neurol 341:289–314.

Alheid GF, de Olmos JS, Beltramino CA. 1995. Amygdala and extended amygdala. In: Paxinos G, editor. The rat nervous system. San Diego: Academic Press. p 495–578.

Arriza JL, Simerly RB, Swanson LW, Evans RM. 1988. The neuronal mineralocorticoid receptor as a mediator of glucocorticoid response. Neuron 1:887–900.

Aston-Jones G, Delfs JM, Druhan J, Zhu Y. 1999. The bed nucleus of the stria terminalis: a target site for noradrenergic actions in opiate withdrawal. Ann NY Acad Sci 877:486–498.

Bayer SA. 1987. Neurogenetic and morphogenetic heterogeneity in the bed nucleus of the stria terminalis. J Comp Neurol 265:47–64.

Beaulieu S, Di Paolo T, Barden N. 1986. Control of ACTH secretion by the central nucleus of the amygdala: implication of the serotoninergic system and its relevance to the glucocorticoid delayed negative feedback mechanism. Neuroendocrinology 44:247–254.

Ben-Ari, Y. 1981. Transmitters and modulators in the amygdaloid complex: a review. In: Ben-Ari Y, editor. The amygdaloid complex. Amsterdam: Elsevier. p 163–174.

Berendse HW, Groenewegen HJ, Lohman AHM. 1992. Compartmental distribution of ventral striatal neurons projecting to the mesencephalon in the rat. J Neurosci 12:2079–2103.

Bernard J-F, Peschanski M, Besson J-M. 1989. A possible spino-(trigemino)-ponto-amygdaloid pathway for pain. Neurosci Lett 100:83–88.

Bernard J-F, Alden M, Besson JM. 1993. The organization of the efferent projections from the pontine parabrachial area to the amygdaloid complex: a *Phaseolus vulgaris*-leucoagglutinin (PHA-L) study in the rat. J Comp Neurol 329:201–229.

Bernard J-F, Huang GF, Besson J-M. 1994. The parabrachial area: electrophysiological evidence for an involvement in visceral nociceptive processes. J Neurophysiol 71:1646–1660.

Bernard J-F, Dallel R, Raboisson P, Villanueva L, Le Bars D. 1995. Organization of the efferent projections from the spinal cervical enlargement to the parabrachial area and periaqueductal grey: a PHA-L study in the rat. J Comp Neurol 353:480–505.

Bester H, Besson J-M, Bernard J-F. 1997a. Organization of efferent projections from the parabrachial area to the hypothalamus: a *Phaseolus vulgaris*-leucoagglutinin study in the rat. J Comp Neurol 383:245–281.

Bester H, Matsumoto N, Besson J-M, Bernard J-F. 1997b. Further evidence for the involvement of the spinoparabrachial pathway in nociceptive processes: a c-Fos study in the rat. J Comp Neurol 383:439–458.

Bittencourt JC, Sawchenko PE. 2000. Do centrally administered neuropeptides access cognate receptors? An analysis in the central corticotropin-releasing factor system. J Neurosci 20:1142–1156.

Bleier R. 1961. The hypothalamus of the cat. A cytoarchitectonic atlas in the Horsley-Clarke coordinate system. Baltimore: Johns Hopkins Press.

Bonaz B, De Giorgio R, Tache Y. 1993. Peripheral bombesin induces c-fos protein in the rat brain. Brain Res 600:353–357.

Bowers G, Cullinan WE, Herman JP. 1998. Region-specific regulation of glutamic acid decarboxylase (GAD) mRNA expression in central stress circuits. J Neurosci 18:5938–5947.

Brady LS, Lynn AB, Herkenham M, Gottesfeld Z. 1994. Systemic interleukin-1 induces early and late patterns of c-fos mRNA expression in brain. J Neurosci 14:4951–4964.

Brog JS, Salyapongse A, Deutch AY, Zahm DS. 1993. The patterns of afferent innervation of the core and shell in the "accumbens" part of the rat ventral striatum: immunohistochemical detection of retrogradely transported fluoro-gold. J Comp Neurol 338:255–278.

Campeau S, Watson SJ. 1997. Neuroendocrine and behavioral response and brain pattern of c-fos induction associated with audiogenic stress. J Neuroendocrinol 9:577–588.

Canteras NS, Swanson LW. 1992. Projections of the ventral subiculum to the amygdala, septum and hypothalamus: a PHAL anterograde tract-tracing study in the rat. J Comp Neurol 324:180–194.

Casada JH, Dafny N. 1991. Restraint and stimulation of bed nucleus of the stria terminalis produce similar stress-like behaviors. Brain Res Bull 27:207–212.

Chan RKW, Vale WW, Sawchenko PE. 2000. Paradoxical activational effects of a corticotropinreleasing factor-binding protein "ligand inhibitor" in rat brain. Neuroscience 101:115–129.

Chen S, Su H-S. 1990. Afferent connections of the thalamic paraventricular and parataenial nuclei in the rat? A retrograde tracing study with iontophoretic application of fluoro-gold. Brain Res 522:1–6.

Cornwall J, Phillipson OT. 1988. Afferent projections to the dorsal thalamus of the rat as shown by retrograde lectin transport. II. The midline nuclei. Brain Res Bull 21:147–161.

Cullinan WE, Herman JP, Battaglia DF, Aki H, Watson SJ. 1995. Pattern and time course of immediate early gene expression in rat brain following acute stress. Neuroscience 64:477–505.

Dallman MF, Akana SF, Cascio CS, Darlington DN, Jacobson L, Levin N. 1987. Regulation of ACTH secretion: variations on a theme of B. Rec Progr Horm Res 43:113–173.

Day HEW, Akil H. 1996. Differential pattern of c-fos mRNA in rat brain following central and systemic administration of interleukin-1-beta: implications for mechanism of action. Neuroendocrinology 63:207–218.

Day HEW, Curran EJ, Watson SJ Jr, Akil H. 1999. Distinct neurochemical populations in the rat central nucleus of the amygdala and bed nucleus of the stria terminalis: evidence for their selective activation by interleukin-1. J Comp Neurol 413:113–128.

Delfs JM, Zhu Y, Druhan JP, Aston-Jones G. 2000. Noradrenaline in the ventral forebrain is critical for opiate withdrawal-induced aversion. Nature 403:430–434.

de Olmos JS. 1972. The amygdaloid projection field in the rat brain as studied with the cupric-silver method. In: Eleftheriou BE, editor. The neurobiology of the amygdala. New York: Plenum. p 145–204.

de Olmos JS, Alheid GF, Beltramino CA. 1985. Amygdala. In: Paxinos G, editor. Forebrain and midbrain. The rat nervous system, vol 1. New York: Academic Press. p 223–334.

Dong H-W, Petrovich GD, Swanson LW. 1999. Organization of the rhomboid nucleus of the BST: a PHAL study in adult rat. Soc Neurosci Abstr 25:2172.

Dong H-W, Petrovich GD, Swanson LW. 2000. Organization of the juxtacapsular nucleus of the BST: a PHAL study in adult rat. Brain Res 859:1–14.

Dong H-W, Petrovich GD, Swanson LW. 2001. Topography of projections from amygdala to the bed nuclei of the stria terminalis. Brain Res Rev (in press).

Dunn AJ, Berridge CW. 1990. Physiological and behavioral responses to corticotropin-releasing factor administration: is CRF a mediator of anxiety or stress responses? Brain Res Rev 15:71–100.

Dunn JD, Williams TJ. 1995. Cardiovascular responses to electrical stimulation of the bed nucleus of the stria terminalis. J Comp Neurol 352:227–234.

Dunn JD. 1987. Plasma corticosterone responses to electrical stimulation of the bed nucleus of the stria terminalis. Brain Res 407:327–331.

Eiden LE, Hökfelt T, Brownstein MJ, Palkovits M. 1985. Vasoactive intestinal polypeptide afferents to the bed nucleus of the stria terminalis in the rat: an immunohistochemical and biochemical study. Neuroscience 15:999–1013.

Ericsson A, Kovács KJ, Sawchenko PE. 1994. A functional anatomical analysis of central pathways subserving the effects of interleukin-1 on stress-related neuroendocrine neurons. J Neurosci 14:879–913.

Fallon JH, Leslie FM. 1986. Distribution of dynorphin and enkephalin peptides in the rat brain. J Comp Neurol 249:293–336.

Freedman LJ, Cassell MD. 1994. Distribution of dopaminergic fibers in the central division of the extended amygdala of the rat. Brain Res 633: 243–252.

Frim DM, Robinson BG, Pasieka KB, Majzoub JA. 1990. Differential regulation of corticotropin-releasing hormone mRNA in rat brain. Am J Physiol 258:E686–E692.

Georges F, Aston-Jones G. 2000. Circuitry linking the bed nucleus of the stria terminalis, nucleus tractus solitarius, and ventral tegmental area: interactions between noradrenergic and dopaminergic systems. Soc Neurosci Abstr 26:1430.

Gerfen CR, Sawchenko PE. 1984. An anterograde neuroanatomical tracing method that shows the detailed morphology of neurons, their axons and terminals: immunohistochemical localization of an axonally transported plant lectin, *Phaseolus vulgaris*-leucoagglutinin (PHA-L). Brain Res 290:219–238.

Gray TS, Magnuson DJ. 1987. Neuropeptide neuronal efferents from the bed nucleus of the stria terminalis and central amygdaloid nucleus to the dorsal vagal complex in the rat. J Comp Neurol 262:365–374.

Gray TS, Magnuson DJ. 1992. Peptide immunoreactive neurons in the amygdala and the bed nucleus of the stria terminalis project to the midbrain central gray in the rat. Peptides 13:451–460.

Gray TS, Peichowski RA, Yracheta JM, Rittenhouse PA, Bethea CL, Van de Kar LD. 1993. Ibotenic acid lesions in the bed nucleus of the stria terminalis attenuate conditioned stress-induced increase in prolactin, ACTH and corticosterone. Neuroendocrinology 57:517–524.

Gritti I, Mainville L, Jones BE. 1994. Projections of GABAergic and cholinergic basal forebrain and GABAergic preoptic-anterior hypothalamic neurons to the posterior lateral hypothalamus of the rat. J Comp Neurol 339:251–268.

Groenewegen HJ, Russchen FT. 1984. Organization of the efferent projections of the nucleus accumbens to pallidal, hypothalamic, and mesencephalic structures: a tracing and immunohistochemical study in the cat. J Comp Neurol 223:347–367.

Groenewegen HJ, Wright CI, Beijer AVJ, Voorn P. 1999. Convergence and segregation of ventral striatal inputs and outputs. Ann NY Acad Sci 877:49–63.

Grove EA. 1988. Neural associations of the substantia innominata in the rat: afferent connections. J Comp Neurol 277:315–346.

Herbert H, Moga MM, Saper CB. 1990. Connections of the parabrachial nucleus with the nucleus of the solitary tract and the medullary reticular formation in the rat. J Comp Neurol 293:540–580.

Herbert H, Forsling ML, Howes SR, Stacey PW, Shiers HM. 1992. Regional expression of c-fos antigen in the basal forebrain following intraventricular infusions of angiotensin and its modulation by drinking either water or saline. Neuroscience 51:867–882.

Herman JP, Cullinan WE. 1997. Neurocircuitry of stress: central control of the hypothalamo-pituitary-adrenocortical axis. Trends Neurosci 20: 78–84.

Herman JP, Cullinan WE, Watson SJ. 1997. Involvement of the bed nucleus of the stria terminalis in tonic regulation of paraventricular hypothalamic CRH and AVP mRNA expression. J Neuroendocrinol 6:43–442.

Hökfelt T, Skirboll L, Rehfeld JF, Goldstein M, Markey K, Dann O. 1980. A subpopulation of mesencephalic dopamine neurons projecting to limbic areas contains a cholecystokinin-like peptide: evidence from immunohistochemistry combined with retrograde tracing. Neuroscience 5:2093–2124.

Holstege G, Meiners L, Tan K. 1985. Projections of the bed nucleus of the stria terminalis to the mesencephalon, pons, and medulla oblongata in the cat. Exp Brain Res 58:379–391.

Johnson AK, de Olmos J, Pastuskovas CV, Zardetto-Smith AM, Vivas L. 1999. The extended amygdala and salt appetite. Ann NY Acad Sci 877:258–280.

Jones BE, Yang T-Z. 1985. The efferent projections from the reticular formation and the locus coeruleus studied by anterograde and retrograde axonal transport in the rat. J Comp Neurol 242:56–92.

Ju G, Han Z-H. 1989. Coexistence of corticotropin releasing factor and neurotensin within oval nucleus neurons in the bed nuclei of the stria terminalis in the rat. Neurosci Lett 99:246–250.

Ju G, Swanson LW. 1989. Studies on the cellular architecture of the bed nuclei of the stria terminalis in the rat: I. Cytoarchitecture. J Comp Neurol 280:587–602.

Ju G, Swanson LW, Simerly RB. 1989. Studies on the cellular architecture of the bed nuclei of the stria terminalis in the rat: II. Chemoarchitecture. J Comp Neurol 280:603–621.

Kay-Nishiyama C, Watts AG. 1998. CRH in dehydration-induced anorexia: CRH immunoreactivity in noncolchicine treated rats, and CRH R2 receptor mRNA levels in the ventromedial hypothalamic nucleus. Soc Neurosci Abstr 24:449.

Kelly AB, Watts AG. 1996. Mediation of dehydration-induced peptidergic gene expression in the rat lateral hypothalamic area by forebrain afferent projections. J Comp Neurol 370:231–246.

Koob GF, Heinrichs SC, Pich EM, Menzaghi F, Baldwin H, Miczek K, Britton KT. 1993. The role of corticotropin-releasing factor in behavioural responses to stress. In: Chadwick DJ, Marsh J, Ackrill K, editors. Corticotropin-releasing factor (Ciba Foundation Symposium 172), Chichester: John Wiley and Sons. p 277–290.

Krettek JE, Price JL. 1978. Amygdaloid projections to subcortical structures within the basal forebrain and the brainstem in the rat and cat. J Comp Neurol 178:225–254.

Lacroix S, Rivest S. 1997. Functional circuitry in the brain of immune-challenged rats: partial involvement of prostaglandins. J Comp Neurol 387:307–324.

Le Gal La Salle G, Paxinos G, Emson P, Ben-Ari Y. 1978. Neurochemical mapping of GABAergic systems in the amygdaloid complex and bed nucleus of the stria terminalis. Brain Res 155:397–403.

Lechner SM, Valentino RJ. 1999. Glucocorticoid receptor-immunoreactivity in corticotrophin-releasing factor afferents to the locus coeruleus. Brain Res 816:17–28.

Lee Y, Davis M. 1997. Role of the hippocampus, the bed nucleus of the stria terminalis and the amygdala in the excitatory effect of corticotropin-releasing hormone on the acoustic startle reflex. J Neurosci 17:6434–6446.

Li BH, Rowland NE. 1995. Effects of vagotomy on cholecystokinin- and dexfenfluramine-induced fos-like immunoreactivity in the rat brain. Brain Res Bull 37:589–593.

Li BH, Spector AC, Rowland NE. 1994. Reversal of dexfenfluramine-induced anorexia and c-fos/c-jun expression by lesion in the lateral parabrachial nucleus. Brain Res 640:255–267.

Loewy AD. 1991. Forebrain nuclei involved in autonomic control. Progr Brain Res 87:253–268.

Luppi P-H, Aston-Jones G, Akaoka H, Chouvet G, Jouvet M. 1995. Afferent projections to the rat locus coeruleus demonstrated by retrograde and anterograde tracing with cholera-toxin B subunit and *Phaseolus vulgaris*-leucoagglutinin. Neuroscience 65:119–160.

Makino S, Gold PW, Schulkin J. 1994. Effects of corticosterone on CRH mRNA and content in the bed nucleus of the stria terminalis; comparison with the effects in the central nucleus of the amygdala and the paraventricular nucleus of the hypothalamus. Brain Res 657:141–149.

Makino S, Shibasaki T, Yamauchi N, Nishioka T, Mimoto T, Wakabayashi I, Gold PW, Hashimoto K. 1999. Psychological stress increased corticotropin-releasing hormone mRNA and content in the central nucleus of the amygdala but not in the hypothalamic paraventricular nucleus in the rat. Brain Res 850:136–143.

Markakis EA, Swanson LW. 1997. Spatiotemporal patterns of secretomotor neuron generation in the parvicellular neuroendocrine system. Brain Res Rev 24:255–291.

McDonald AJ. 1998. Cortical pathways to the mammalian amygdala. Progr Neurobiol 55:257–332.

McDonald AJ, Shammah-Lagnado SJ, Shi CJ, Davis M. 1999. Cortical afferents to the extended amygdala. Ann NY Acad Sci 877:309–338.

Moga MM, Gray TS. 1985. Evidence for corticotropin-releasing factor, neurotensin, and somatostatin in the neural pathway from the central nucleus of the amygdala to the parabrachial nucleus. J Comp Neurol 241:275–284.

Moga MM, Saper CB. 1994. Neuropeptide-immunoreactive neurons projecting to the paraventricular hypothalamic nucleus in the rat. J Comp Neurol 346:137–150.

Moga MM, Saper CB, Gray TS. 1989. Bed nucleus of the stria terminalis: cytoarchitecture, immunohistochemistry, and projection to the parabrachial nucleus in the rat. J Comp Neurol 283:315–332.

Moga MM, Herbert H, Hurley KM, Yasui Y, Gray TS, Saper CB. 1990. Organization of cortical, basal forebrain, and hypothalamic afferents to the parabrachial nucleus in the rat. J Comp Neurol 295:624–661.

Moga MM, Weis RP, Moore RY. 1995. Efferent projections of the paraventricular thalamic nucleus in the rat. J Comp Neurol 359:221–238.

Mogenson GJ, Swanson LW, Wu M. 1985. Evidence that projections from substantia innominata to zona incerta and mesencephalic locomotor region contribute to locomotor activity. Brain Res 334:65–76.

Moore RY. 1978. Catecholamine innervation of the basal forebrain. I. The septal area. J Comp Neurol 177:665–684.

Morin LP, Goodless-Sanchez N, Smale L, Moore RY. 1994. Projections of the suprachiasmatic nuclei, subparaventricular zone and retrochiasmatic area in the golden hamster. Neuroscience 61:391–410.

Nitecka L, Ben-Ari Y. 1987. Distribution of GABA-like immunoreactivity in the rat amygdaloid complex. J Comp Neurol 266:45–55.

Nunez AA, Bult A, McElhinny TL, Smale L. 1999. Daily rhythms of Fos expression in hypothalamic targets of the suprachiasmatic nucleus in diurnal and nocturnal rodents. J Biol Rhythms 14:300–306.

Oertel WH, Riethmuller G, Mugnaini E, Schmechel DE, Weindl A, Gramsch C, Herz A. 1983. Opioid peptide-like immunoreactivity localized in GABAergic neurons of rat neostriatum and central amygdaloid nucleus. Life Sci 1:73–76.

Palkovits M, Epelbaum J, Gros C. 1981. Met-enkephalin concentrations in individual brain nuclei of ansa lenticularis and stria terminalis transected rats. Brain Res 216:203–209.

Paxinos G, Watson C. 1986. The rat brain in stereotaxic coordinates, 2nd ed. Sydney: Academic Press.

Paxinos G, Watson C. 1998. The rat brain in stereotaxic coordinates, 3rd ed. San Diego: Academic Press.

Petrovich GD, Swanson LW. 1997. Projections from the lateral part of the central amygdalar nucleus to the postulated fear conditioning circuit. Brain Res 763:247–254.

Petrovich GD, Scicli AP, Thompson RF, Swanson LW. 2000. Associative fear conditioning of enkephalin mRNA levels in central amygdalar neurons. Behav Neurosci 114:681–686.

Peyron C, Petit J-M, Rampon C, Jouvet M, Luppi P-H. 1998. Forebrain afferents to the rat dorsal raphe nucleus demonstrated by retrograde and anterograde tracing methods. Neuroscience 82:443–468.

Phelix CF, Liposits Z, Paull WK. 1992a. Serotonin-CRF interaction in the bed nucleus of the stria terminalis: a light microscopic double-label immunocytochemical analysis. Brain Res Bull 28:943–948.

Phelix CF, Liposits Z, Paull WK. 1992b. Monoamine innervation of bed nucleus of stria terminalis: an electron microscopic investigation. Brain Res Bull 28:949–965.

Pickel VM, Segal M, Bloom FE. 1974. A radioautographic study of the efferent pathways of the nucleus locus coeruleus. J Comp Neurol 155: 15–42.

Rao ZR, Yamano M, Shiosaka S, Shinohara A, Tohyama M. 1987. Origin of leucine-enkephalin fibers and their two main afferent pathways in the bed nucleus of the stria terminalis in the rat. Exp Brain Res 65:411–420.

Ricardo UA, Koh ET. 1978. Anatomical evidence of direct projections from the nucleus of the solitary tract to the hypothalamus, amygdala, and other forebrain structures in the rat. Brain Res 153:1–26.

Riche D, De Pommery J, Menetrey D. 1990. Neuropeptides and catecholamines in efferent projections of the nucleus of the solitary tract in the rat. J Comp Neurol 293:399–424.

Risold PY, Swanson LW. 1997. Chemoarchitecture of the rat lateral septal nucleus. Brain Res Rev 24:91–113.

Risold PY, Thompson RH, Swanson LW. 1997. The structural organization of connections between hypothalamus and cerebral cortex. Brain Res Rev 24:197–254.

Roder S, Ciriello J. 1994. Collateral axonal projections to limbic structures from ventrolateral medullary A1 noradrenergic neurons. Brain Res 638:182–188.

Roozendaal B, Koolhaas JM, Bohus B. 1991. Attenuated cardiovascular, neuroendocrine, and behavioral responses after a single footshock in central amygdaloid lesioned male rats. Physiol Behav 50:771–775.

Ross CA, Ruggiero DA, Reis DJ. 1985. Projections from the nucleus tractus solitari to the rostral ventrolateral medulla. J Comp Neurol 242:511–534.

Rowland NE, Li B-H, Rozelle AK, Fregly MJ, Garcia M, Smith GC. 1994. Localization of changes in immediate early gene in brain in relation to hydromineral balance: intravenous angiotensin II. Brain Res Bull 33: 427–436.

Rowland NE, Bllinger LL, Li BH, Mendel VE. 1996. Satietin: Fos mapping of putative brain sites of action. Brain Res 717:189–192.

Saper CB. 1982. Convergence of autonomic and limbic connections in the insular cortex of the rat. J Comp Neurol 210:163–173.

Saper CB, Loewy AD. 1980. Efferent connections of the parabrachial nucleus in the rat. Brain Res 197:291–317.

Satoh K, Fibiger HC. 1986. Cholinergic neurons of the laterodorsal tegmental nucleus: efferent and afferent connections. J Comp Neurol 253:277–302.

Sawchenko PE, Swanson LW. 1983. The organization of forebrain afferents to the paraventricular and supraoptic nuclei of the rat. J Comp Neurol 218:121–144.

Schwaber JS, Kapp BS, Higgins EA, Rapp PR. 1982. Amygdaloid and basal forebrain direct connections with the nucleus of the solitary tract and the dorsal motor nucleus. J Neurosci 2:1424–1438.

Senba E, Ueyama T. 1997. Stress-induced expression of immediate early genes in the brain and peripheral organs of the rat. Neurosci Res 29:183–207.

Shimada S, Inagaki S, Kubota Y, Ogawa N, Shibasaki T, Takagi H. 1989. Coexistence of peptides (corticotropin releasing factor/neurotensin and substance P/somatostatin) in the bed nucleus of the stria terminalis and central amygdaloid nucleus of the rat. Neuroscience 30:377–383.

Simerly RB, Swanson LW. 1989. Projections of the medial preoptic nucleus: a *Phaseolus vulgaris*-leucoagglutinin anterograde tract-tracing study in the rat. J Comp Neurol 270:209–242.

Simerly RB, Chang M, Muramatsu M, Swanson LW. 1990. Distribution of

androgen and estrogen receptor mRNA-containing cells in the rat brain: an in situ hybridization study. J Comp Neurol 294:76–95.

Sofroniew MV. 1983. Direct reciprocal connections between the bed nucleus of the stria terminalis and dorsomedial medulla oblongata: evidence from immunohistochemical detection of tracer proteins. J Comp Neurol 213:399–405.

Spooren WPJM, Veening JG, Cools AR. 1993. Descending connections of the sub-pallidal areas in the cat: projections to the subthalamic nucleus, the hypothalamus, and the midbrain. Synapse 15:104–123.

Steriade M, Datta S, Pare D, Oakson G, Dossi RC. 1990. Neuronal activities in brainstem cholinergic nuclei related to tonic activation processes in thalamocortical systems. J Neurosci 10:2541–2559.

Sun N, Cassell MD. 1993. Intrinsic GABAergic neurons in the rat central extended amygdala. J Comp Neurol 330:381–404.

Sun N, Roberts L, Cassell MD. 1991. Rat central amygdaloid nucleus projections to the bed nucleus of the stria terminalis. Brain Res Bull 27:651–662.

Sun N, Yi H, Cassell MD. 1994. Evidence for a GABAergic interface between cortical afferents and brainstem projection neurons in the rat central extended amygdala. J Comp Neurol 340:43–64.

Swanson CJ, Kalivas P. 2000. Regulation of locomotor activity by metabotropic glutamate receptors in the nucleus accumbens and ventral tegmental area. J Pharmacol Exp Ther 292:406–414.

Swanson LW. 1987. The hypothalamus. In: Björklund A, Hökfelt T, Swanson LW, editors. Handbook of chemical neuroanatomy. Integrated systems of the CNS, part I. Amsterdam: Elsevier. p 1–124.

Swanson LW. 1991. Biochemical switching in hypothalamic circuits mediating responses to stress. Progr Brain Res 87:181–200.

Swanson LW. 1999. Brain maps: structure of the rat brain, 2nd ed. Amsterdam: Elsevier.

Swanson LW. 2000. Cerebral hemisphere regulation of motivated behavior. Brain Res 886:113–164.

Swanson LW, Cowan WM. 1979. The connections of the septal region in the rat. J Comp Neurol 186:621–665.

Swanson LW, Lind RW. 1986. Neural projections subserving the initiation of a specific motivated behavior in the rat: new projections from the subfornical organ. Brain Res 379:399–403.

Swanson LW, Petrovich GD. 1998. What is the amygdala? Trends Neurosci 21:323–331.

Swanson LW, Simmons DM. 1989. Differential steroid hormone and neural influences on peptide mRNA levels in CRH cells of the paraventricular nucleus: a hybridization histochemical study in the rat. J Comp Neurol 285:413–435.

Swanson LW, Mogenson GJ, Gerfen CR, Robinson P. 1984. Evidence for a projection from the lateral preoptic area and substantia innominata to the "mesencephalic locomotor region." Brain Res 295:161–178.

Terenzi MG, Ingram CD. 1995. A combined immunocytochemical and retrograde tracing study of noradrenergic connections between the caudal medulla and bed nuclei of the stria terminalis. Brain Res 672: 289–297.

Thompson RH, Swanson LW. 1998. Organization of inputs to the dorsomedial nucleus of the hypothalamus: a reexamination with fluorogold and PHAL in the rat. Brain Res Rev 27:89–118.

Thompson RH, Canteras NS, Swanson LW. 1996. Organization of projections from the dorsomedial nucleus of the hypothalamus: a PHA-L study in the rat. J Comp Neurol 376:143–173.

Thrivikraman KV, Nemeroff CB, Plotsky PM. 2000. Sensitivity to glucocorticoid-mediated fast-feedback regulation of the hypothalamic-pituitary-adrenal axis is dependent upon stressor specific neurocircuitry. Brain Res 870:87–101.

Uhl GR, Snyder SH. 1979. Neurotensin: a neuronal pathway projecting from amygdala through stria terminalis. Brain Res 161:522–526.

Veening JG, Swanson LW, Sawchenko PE. 1984. The organization of projections from the central nucleus of the amygdala to brainstem sites involved in central autonomic regulation: a combined retrograde transport-immunohistochemical study. Brain Res 303:337–357.

Veinante P, Stoeckel M-E, Freund-Mercier M-J. 1997. GABA- and peptide-immunoreactivities co-localize in the rat central extended amygdala. Neuroreport 8:2985–2989.

Vertes RP. 1990a. Fundamentals of brainstem anatomy: a behavioral perspective. In Klemm WR, Vertes RP, editors. Brainstem mechanisms of behavior. New York: John Wiley and Sons. p 33–103.

Vertes RP. 1990b. Brainstem mechanisms of slow-wave sleep and REM sleep. In Klemm WR, Vertes RP, editors. Brainstem mechanisms of behavior. New York: John Wiley and Sons. p 535–583.

Vertes RP. 1991. A PHA-L analysis of ascending projections of the dorsal raphe nucleus in the rat. J Comp Neurol 313:643–668.

Von Krosigk M, Smith AD. 1990. Descending projections from the substantia nigra and retrorubral field to the medullary and pontomedullary reticular formation. Eur J Neurosci 3:260–273.

Wang P-Y, Zhang F-Z. 1995. Outlines and atlas for learning rat brain slides [in Chinese]. China: Northwest University Press.

Watts AG. 2000. Understanding the neural control of ingestive behaviors: helping to separate cause from effect with dehydration-associated anorexia. Horm Behav 37:261–283.

Watts AG. 2001. Neuropeptides and the integration of motor responses to dehydration. Annu Rev Neurosci 24:357–384.

Watts AG, Sanchez-Watts G. 1995. Region-specific regulation of neuropeptide mRNAs in rat limbic forebrain neurones by aldosterone and corticosterone. J Physiol 484:721–736.

Watts AG, Swanson LW, Sanchez-Watts G. 1987. Efferent projections of the suprachiasmatic nucleus: I. Studies using anterograde transport of *Phaseolus vulgaris*-leucoagglutinin in the rat. J Comp Neurol 258:204–229.

Watts AG, Kelly AB, Sanchez-Watts G. 1995. Neuropeptides and thirst: the temporal response of corticotropin-releasing hormone and neurotensin/neuromedin gene expression in rat limbic forebrain neurons to drinking hypertonic saline. Behav Neurosci 109:1146–1157.

Weller KL, Smith DA. 1982. Afferent connections to the bed nucleus of the stria terminalis. Brain Res 232:255–270.

Woulfe JM, Hrycyshyn AW, Flumerfelt BA. 1988. Collateral axonal projections from the A1 noradrenergic cell group to the paraventricular nucleus and bed nucleus of the stria terminalis in the rat. Exp Neurol 102:121–124.

Yasui Y, Breder CD, Saper CB, Cechetto DF. 1991. Autonomic responses and efferent pathways from the insular cortex in the rat. J Comp Neurol 303:355–374.

Zagon A, Totterdell S, Jones RSG. 1994. Direct projections from the ventrolateral medulla oblongata to the limbic forebrain: anterograde and retrograde tract-tracing studies in the rat. J Comp Neurol 340:445–468.